SHOCK WAVES IN CHEMICAL KINETICS

Thesis by

John Doyle Britton

In Partial Fulfillment of the Requirements

for the Degree of

Doctor of Philosophy

California Institute of Technology

Pasadena, California

1955

Acknowledgements

I would like to thank Professor Norman Davidson for supervising what was an extremely pleasant and instructive period of time. I would also like to thank the many faculty members, employees, and fellow students who were ever ready with aid and advice.

The receipt of assistantships or fellowships from the California Institute, E. I. du Pont de Nemours and Co., Inc., and the National Science Foundation is gratefully acknowledged. The research was supported by the Office of Naval Research.

Abstract

The rates of dissociation of I_2 in N_2 and CO_2, and Br_2 in A were measured at temperatures around 1300°K by heating room temperature mixtures by means of shock waves and observing the subsequent reactions. The rates of recombination of both I_2 and Br_2 were found to decrease with increasing temperature. The results, combined with room temperature measurements seemed to be best expressed in the form $k_R = A \exp(E/RT)$. Attempts to measure the efficiency of I_2 or Br_2 molecules as third bodies for the recombination gave only rather wide limits to the possible values.

The experiments also showed that CO_2 is vibrationally relaxed at high temperatures in a time short compared to the reaction time of 20-200 microseconds. It was not possible to decide whether or not N_2 is vibrationally relaxed at this temperature in this short time.

Extinction coefficients of I_2 and Br_2 were measured as a function of the temperature. They appeared to be dependent on the inert gas.

Table of Contents

Introduction

A shock wave is a steep fronted pressure wave. It provides a means by which gases can be compressed and heated in a time of the order of a few collision times for the molecules. Thus it is possible to heat a gas to a non-equilibrium situation if the gas is one that can undergo some reaction at higher temperatures. The heating that takes place represents a change in the translational energy of the gas. Molecular rotation is excited nearly as fast as the translation, that is, in the front of the shock wave itself, and too fast to be detected by the means described below. The excitation of vibrational energy, also referred to as vibrational relaxation, sometimes occurs nearly as fast as rotational excitation and therefore too fast to detect, and sometimes occurs too slowly to detect, and of course at all rates between. A chemical reaction, in which the molecular species change, is also possible, and may occur at a rate anywhere from too slow to be measured to too fast to be measured. If it is possible to follow some characteristic of the gas behind a shock wave as a function of the time then it may be possible to study the kinetics of a reaction occurring in the gas.

The first chemical reaction to be studied by this method was the dissociation of N_2O_4 into NO_2 (1), which occurs at a measurable rate near room temperature. It was studied by following the change in the color of the gas. At the wavelength of light used the color was due to NO_2 and therefore provided a direct means of following the NO_2 concentration. As the

second test of the method it was decided to study the rate of dissociation of I_2 into atoms (2). This reaction is essentially the same as the N_2O_4-NO_2 reaction except that it occurs at higher temperatures, around 1300°K. It was of additional interest because the rate of recombination of I atoms into molecules had been studied at room temperature by flash photolysis techniques, and the high temperature results would provide an extension of this work. After the work on I_2 was well under way it was decided to study the dissociation of Br_2 as well.

This thesis describes some of the work done to date on I_2 and Br_2 dissociation.

Shock Wave Behavior

From the equations of state for a particular gas and the assumption of conservation of mass, momentum, and energy across a shock wave the conditions in a shock wave can be calculated. The equations describing the behavior of a shock wave have been derived in the literature a number of times, but they are rederived here (Appendix B) in a form more convenient for calculations. The derivation is in the spirit of the treatment by Döring (3).

The number of parameters required to describe a shock wave and the physical restrictions on these parameters are such that if any one parameter is determined and the initial conditions are known then all the parameters of the shock wave are determined. The parameter that is measured in order to determine the behavior behind the shock wave is the velocity.

If there is a reaction behind the shock front then the conditions are determined for any given amount of reaction. They are not known for a particular point behind the shock front because to know this one would need to know the rate of the reaction. Measuring the rate of a reaction behind a shock wave involves measuring the change in some property of the gas as a function of distance (and also therefore of time) behind the shock wave, and comparing this with the calculated change in this property as a function of the amount of reaction.

The behavior of various properties of certain gases is shown, semi-quantitatively as a function of distance behind the shock wave, in figure 1. It can be seen from these curves that pressure would be a poor parameter to measure in any case. Density would be rather good if vibrational relaxation or the dissociation of pure I_2 were being studied. It is also apparent that the dissociation of pure I_2 in a shock wave is highly non-isothermal, and that in order to approximate isothermal conditions it is best to use a large percentage of inert gas to act as a heat capacity buffer. In this case the density also changes little and I_2 concentration is a much better parameter to measure. This is what is done.

The Shock Tube

The shock tube is a device for producing uniform shock waves. In its simplest form it consists of a tube which can be separated into two sections by an easily ruptured diaphragm. Into one section gas at high pressure, called the driving gas, is introduced. Into the other section the gaseous reaction

Figure 1 Behavior Behind the Shock

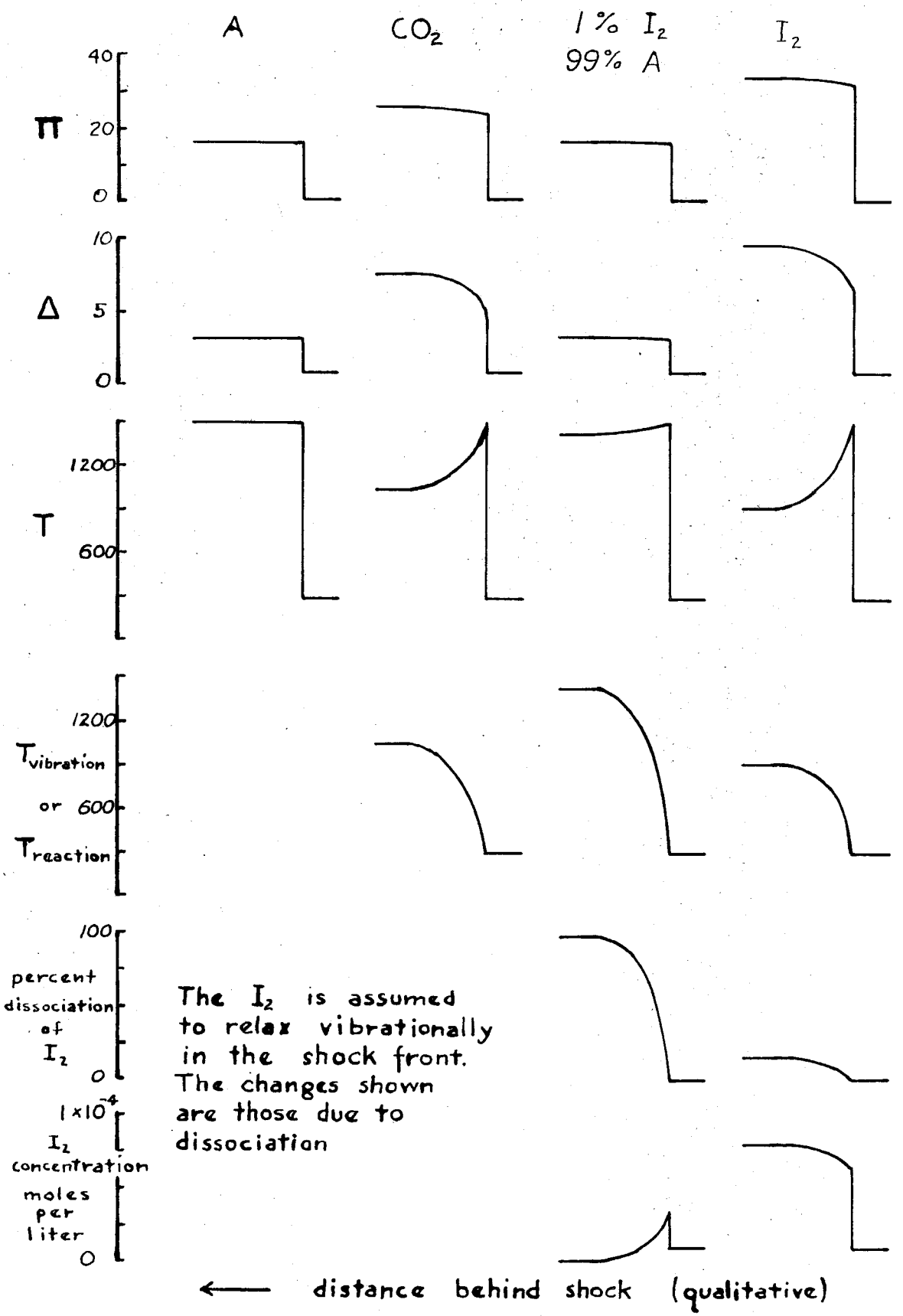

mixture, at low pressure, is introduced. To produce a shock wave the diaphragm is ruptured and the high pressure driving gas allowed to expand. This compresses the low pressure gas and drives it down the tube. The steep pressure front of this moving compressed gas is the shock wave. It is steep fronted because the gas behind it is heated when it is compressed, and any pressure increments travel to the shock front at the speed of sound in the heated gas plus the speed of the gas moving behind the shock wave. This speed is always greater than the speed of the shock wave itself, so that any pressure increments catch up with the shock front eventually.

A shock tube and the pressure configurations in the shock tube at several times during the course of the shock wave are shown in figure 2.

The Apparatus and the Experimental Procedure

The shock tube and the various detecting and measuring arrangements are shown schematically in figure 2. Figures 3ab and 4ab are photographs of the apparatus from various angles. They will be referred to as the different features of the apparatus are discussed.

The tube was of uniform 15 cm inside diameter. Two sections for the driving gas were available, one 182 cm long, and the other 31 cm long. The driving section was connected to a manifold through which the tube could be evacuated and filled with any desired driving gas and the pressure measured. The driving section was mounted on rollers so that it could be moved away from the low pressure section to allow the mounting

Figure 2 Diagram of the Apparatus Pressure Profiles in a Shock Tube

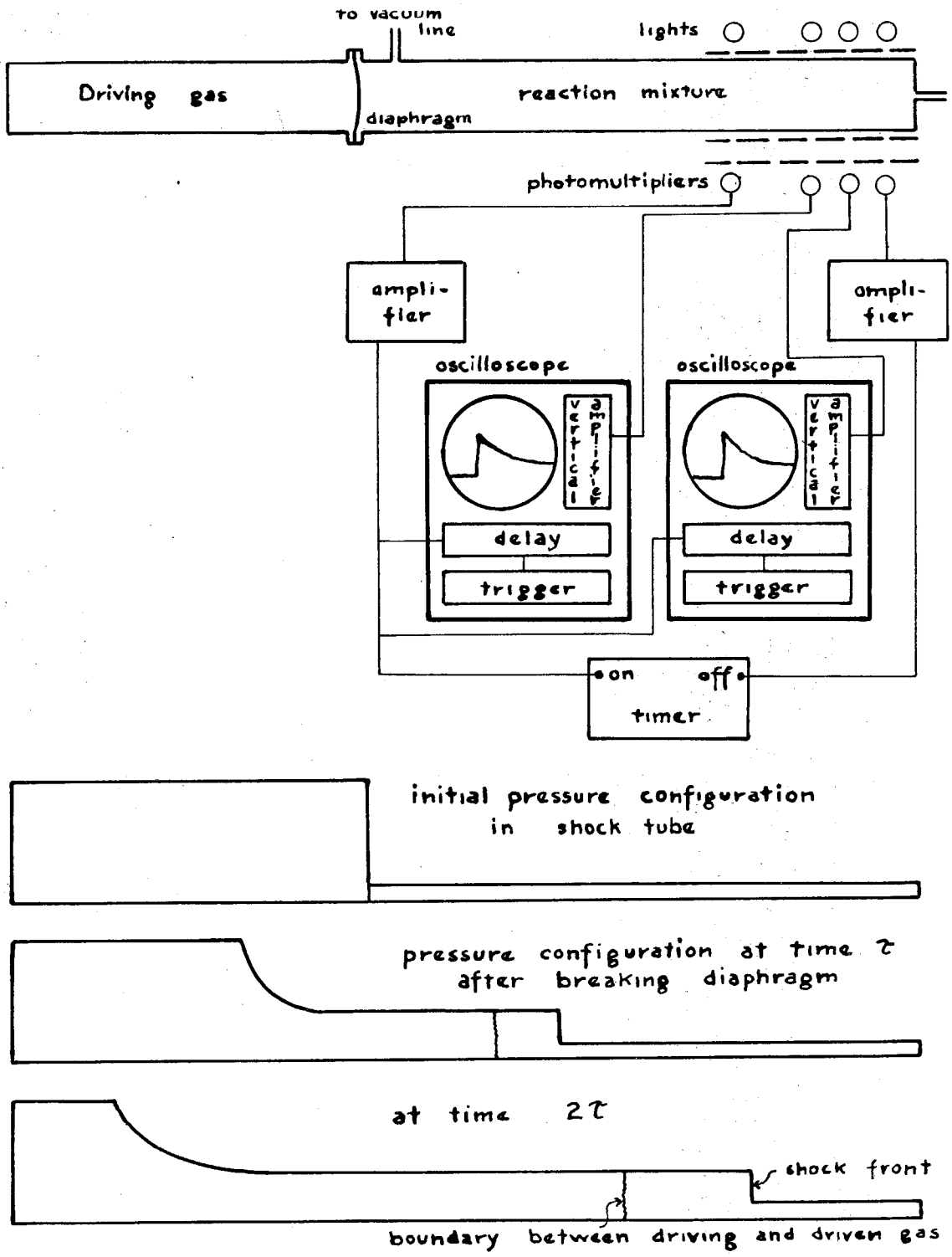

Figure 3

3a View from south, same orientation as figure 2

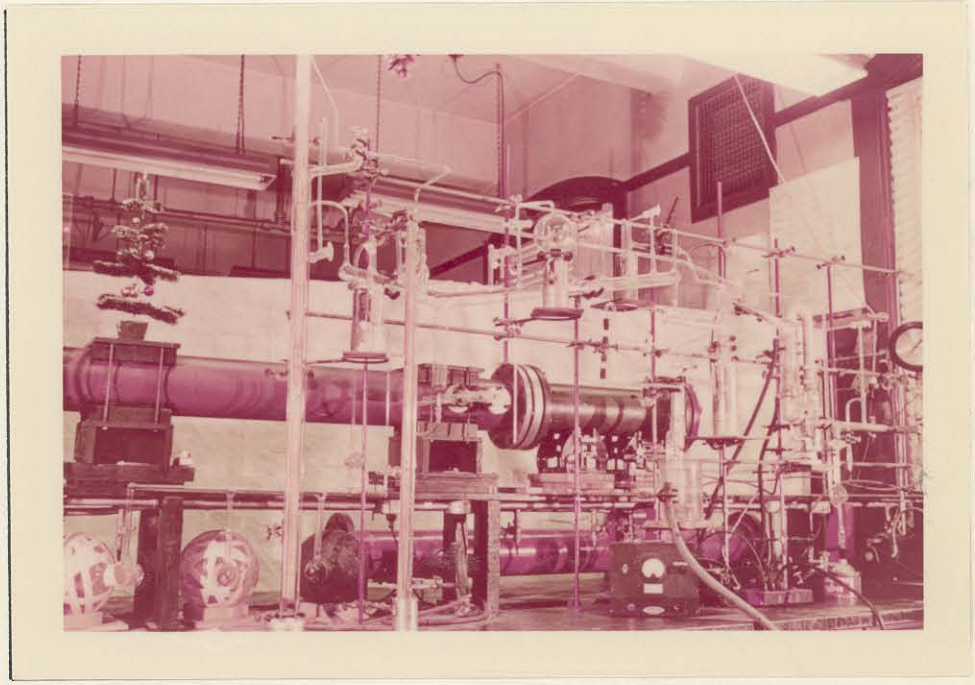

3b View from north, showing vacuum line and high pressure end

Figure 4

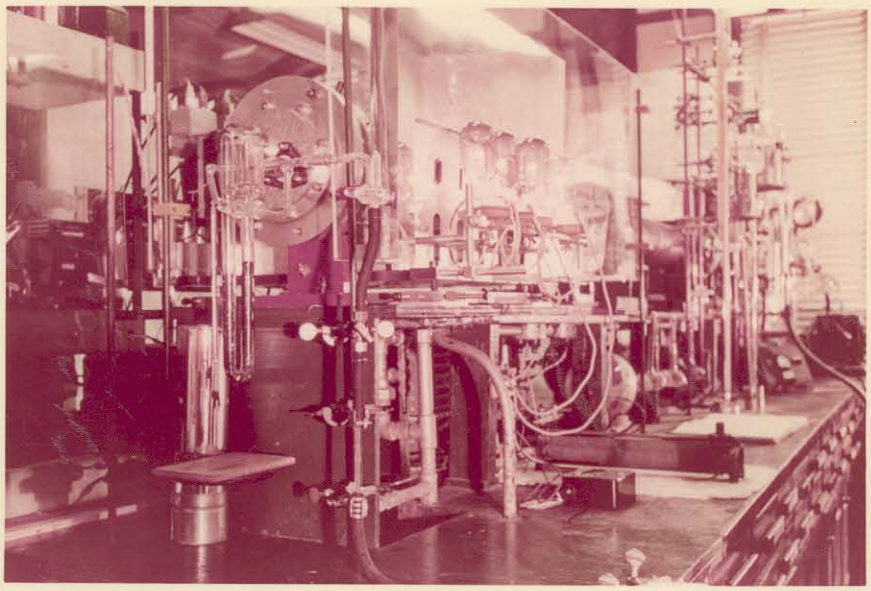

4a View from east, showing low pressure end, light sources, and iodine saturator

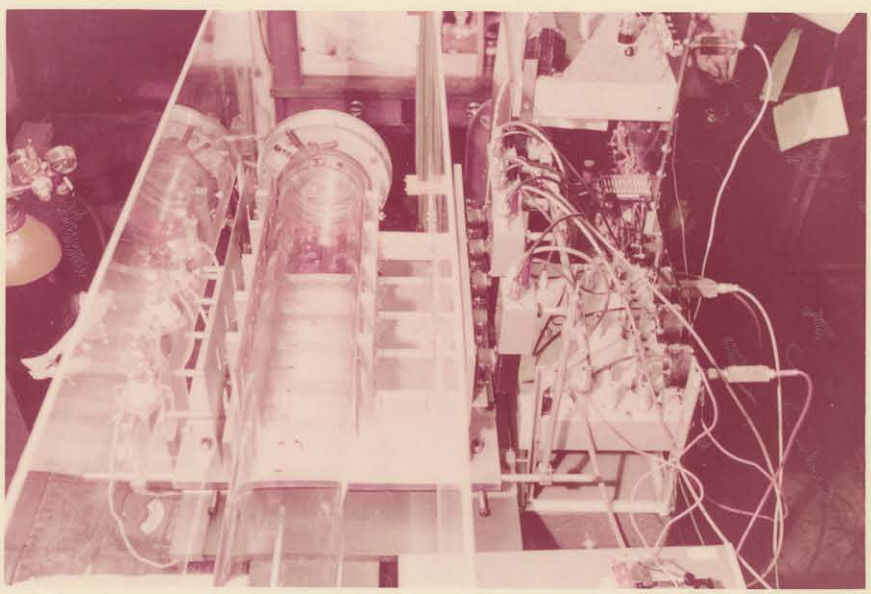

4b View from west above, looking down towards low pressure end, showing optical bench and light arrangement

of the diaphragm. All this can be seen in figures 3a and 3b.

The diaphragms were sheets of cellulose acetate of thicknesses from 0.003 in. to 0.030 in. They were clamped between the driving section and the low pressure section in a device which allowed them to be broken by a needle if necessary. There is a certain amount of turbulence at the first due to the breaking of the diaphragm. Presumably if the diaphragm broke poorly, that is, slowly or into large fragments, there could be so much turbulence that the region behind the shock would not be uniform when the shock passed the observation stations. It was observed that even when the diaphragms were broken at one-half their spontaneous breaking pressure there was no evidence that the shocks were any different from the usual ones. However, looking through a fifteen centimeter light path one might not see turbulence if it were on a very small scale or confined to a small layer near the walls.

The low pressure section was 292 cm long. It consisted of a 140 cm aluminum section next to the high pressure end and a 152 cm section of Pyrex pipe through which observations were made. Two different methods were used to fill the low pressure section with the reaction mixture. For mixtures including I_2 the inert gas was flowed through a 15 cm tube filled with I_2 crystals, which was held at a fixed temperature. This device can be seen in figure 4a. It determined the pressure of I_2 and the pressure of the total mixture was measured as the gas flowed out of the shock tube. The flow was from right to left in figure 2, and served to sweep the tube free of

other gases as well as saturate with I_2. For mixtures involving Br_2 the mixture was made up in bulbs on the vacuum line and stored. The tube was evacuated until just before the shock was to be run and then filled to the desired pressure with the mixture. The low pressure section could be evacuated to less than 1 micron pressure, and leaked or degassed at about 0.1 micron per minute.

The arrangement used to study any reactions behind the shock wave was to observe the colored gases spectrophotometrically at various points along the shock tube. Light from a 500 watt tungsten projection lamp operated at 120 volts d.c., or from a Hanovia medium pressure d.c. mercury arc, Sc 5031, was used. The light from the source, 17 cm from the tube, was passed through a slit 1 cm from the tube, through the tube, through another slit 1 cm from the tube, through another slit 16 cm from the tube, and onto the photomultiplier, 9 cm further on. The photomultipliers were RCA 931's. The light arrangement can be seen in figure 4b. Filters were used to limit the light present. they will be discussed more fully in the sections on extinction coefficients.

A simple optical bench was constructed in order to align the lights, slits, photomultipliers, and tube as well as possible. The following tolerances were achieved. The distance between successive slits was 10.000 ± 0.005 cm. The distances between any particular set of pairs of slits on the three different slit systems was the same to 0.0005 cm. The slits were perpendicular to the axis of the tube to within an angle of 5'.

The plane containing the successive slits was parallel to the axis of the tube to within an angle of 10'. The inside and outside diameters of the tube were measured at various points along the tube. These measurements are shown in figure 5. The walls of the tube are uniform but the diameter varies by about 0.1 cm in 100 cm. The maximum angular variation in the diameters is about 15'.

These alignments were made because some results from early experiments seemed to indicate a lack of alignment and hence a loss of resolving time. This was indicated by the time it took the steep front of the shock wave to rise its full height on the oscilloscope trace. If one observed the passage of a shock front at 100 cm/msec velocity past a 0.10 cm slit system, through which, by perfect alignment, a sheet of light 0.10 cm thick ~~were~~ was passing parallel to the shock front, it would take the shock front 1 microsecond to rise to its full height. Some experiments showed a time of rise of 5-7 microseconds. The optical system described was constructed in which, with the limits of error given, and the arrangement of slits, lights, and photomultipliers described, the same shock should have a rise time of less than 3 microseconds. The long times of rise still occurred in some of the shocks. This indicated either that the shock fronts were curved or that they were not normal to the walls of the tube. In figure 7b an oscilloscope trace displaying this slow rise is reproduced.

As indicated in figure 2 signals from the photomultipli-

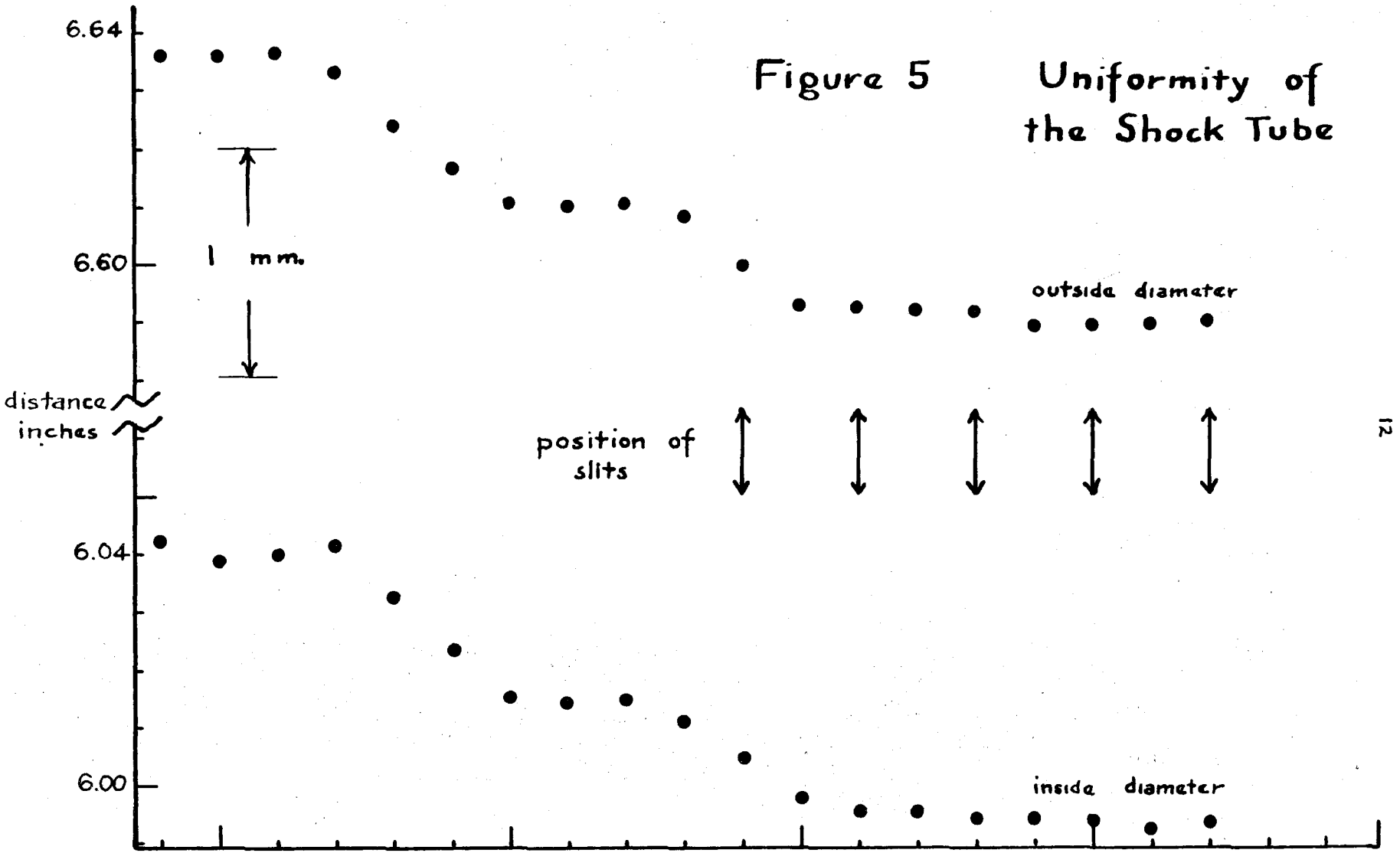

Figure 5 Uniformity of the Shock Tube

ers at either end went to a timer, a Potter Model 456 1.6 Megacycle Counter Chronograph. This determined the time for the shock to pass between these two stations to an accuracy of 0.63 microseconds. The signal from the initial station also served to begin the oscilloscope sweeps.

Signals from the two middle photomultipliers were displayed directly on two different oscilloscopes. That two oscilloscopes were available made it possible to observe the shock wave at two different wavelengths of light or at two different writing rates on the oscilloscopes. The time scale was put on the oscilloscope by putting a signal from a 100 kc crystal controlled oscillator onto an intensifying electrode in the cathode ray tube, and blanking 1 microsecond of the sweep in every 10. Vertical deflection calibrations were put on with a battery and a Helipot precision potentiometer. The oscilloscope traces were photographed, and measurements were made on enlarged projections from the negatives.

Figures 6ab, 7ab, and 8ab show various types of oscilloscope traces. Figure 6a is the record of a shock wave in a CO_2-I_2 mixture at a temperature low enough that no reaction takes place. Figure 7a shows the dissociation of Br_2 proceeding at a measurable rate. Figures 8a and 8b show the same shock wave recorded at two different writing rates on the two oscilloscopes. In figure 8b the reaction can be seen to proceed up to the cold front, that is, the boundary between the driving gas and the driven gas, at which point there is a sudden decrease in the Br_2 concentration.

Figure 6

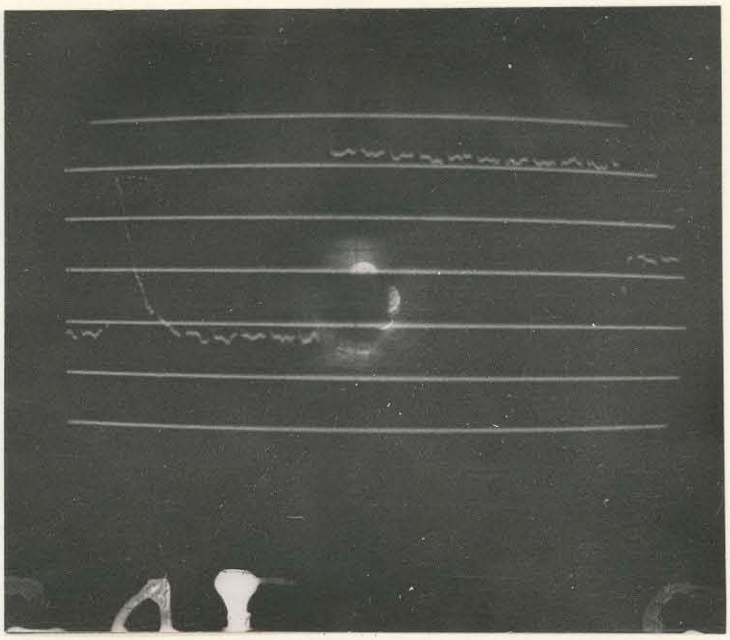

6a Shock wave in CO_2 (0.45% I_2). Temperature 736°K assuming CO_2 relaxed. Initial concentration 2.14 x 10^{-3} mole/liter. Compression ratio 5.83. The spike at the left side of the picture is related to the timing, and can be ignored.

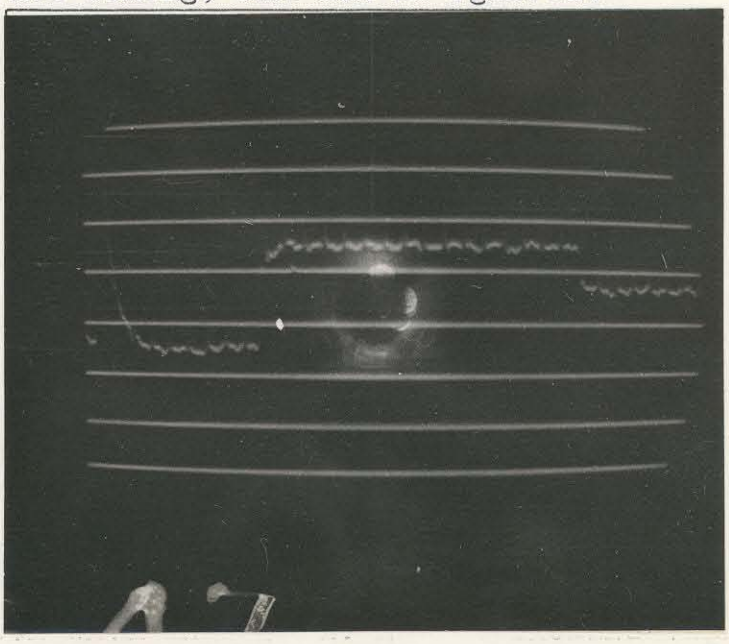

6b Shock wave in CO_2 (1.21% I_2) showing vibrational relaxation of CO_2. Temperature 573°K before relaxation, 500°K after. Initial concentration 0.615 mole/liter. Compression ratio 3.63-3.73 (final).

Figure 7

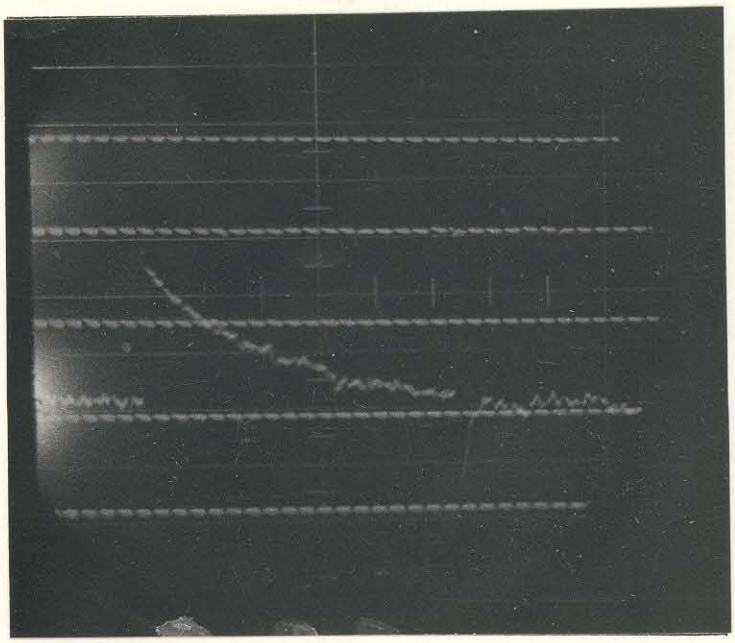

7a Shock wave in A (1% Br_2). Temperature 1490°K before reaction, about 1412°K after. Note sharp rise of signal at front of shock wave, about 2 microseconds.

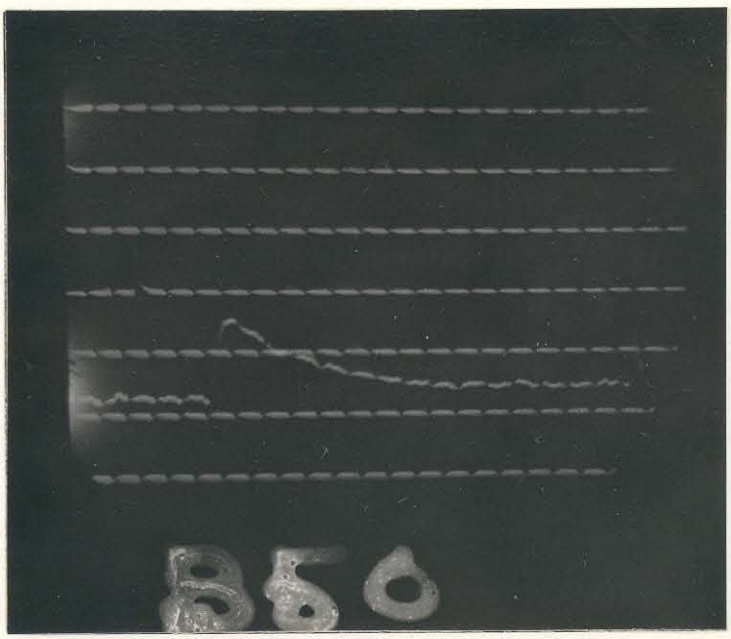

7b Shock in A (10% Br_2). Temperature 2130°K before reaction. Note slow rise of signal at front of shock wave, about 7 microseconds, when 2 to 3 would be expected. This suggests curved shock front, or plane front not perpendicular to the walls of the tube.

Figure 8

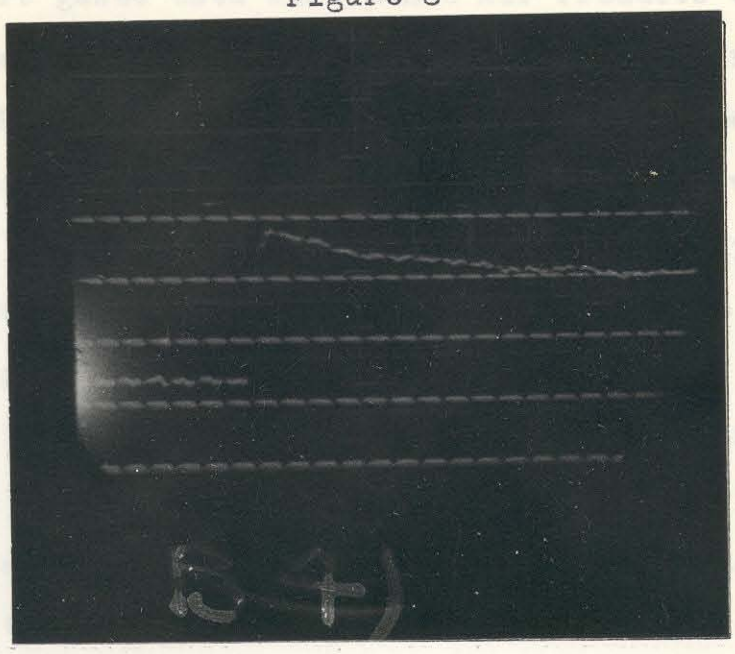

8a Shock wave into A (10% Br_2). Initial temperature 1767°K. Writing rate of oscilloscope 20 microseconds per centimeter.

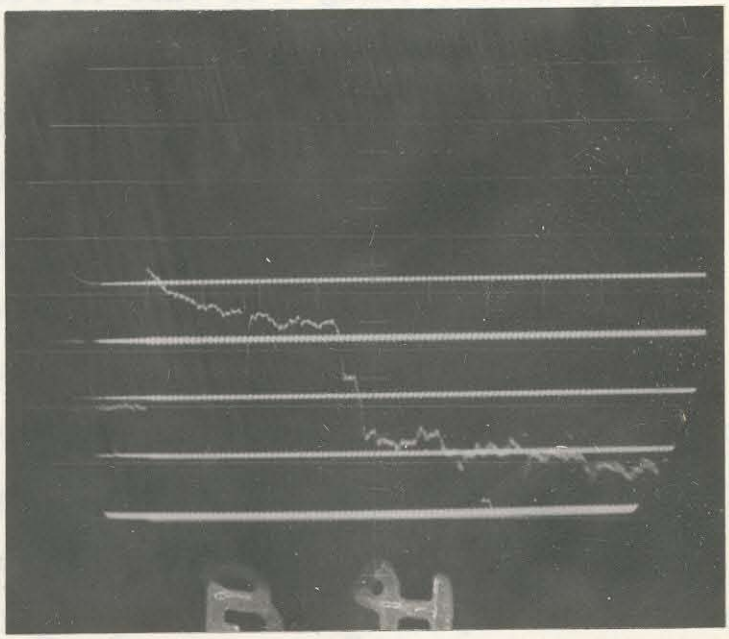

8b Same shock wave as 8a. Writing rate of oscilloscope 100 microseconds per centimeter. Note cold front about 350 microseconds after shock front.

The inert gases used were Linde Air Products Co. argon, said to be better than 99.8% pure, Linde pure dry nitrogen, said to be 99.90% pure, and carbon dioxide supplied by Pure Carbonics Incorporated and said to be 99.5% pure, with impurities air and water. The I_2 used was 'Baker's Analyzed' Reagent. The Br_2 was Merck Reagent Grade. Both were used without further purification.

In the I_2 experiments the inert gas flowed through a regulator at a few pounds pressure above atmospheric, through a flowmeter at the rate of about 500 cc/min, through a needle valve where the pressure dropped to the experimental value, over the I_2, and through the shock tube. The gas mixture entered the shock tube at the downstream end and left near the diaphragm where it went to a glass vacuum apparatus in which the pressure could be measured on a dibutyl-phthalate manometer. It left the vacuum line through a needle valve and went to a pump. The two needle valves were the only significant constrictions in the system. Since there were no important constrictions between the two needle valves the pressure in the whole system could be assumed uniform, and a measurement of the pressure in the manometer on the glass vacuum line was a correct measurement of the pressure of the gas flowing through the shock tube.

In the Br_2 experiments Br_2 was put into evacuated bulbs to the desired pressure which was measured on the dibutyl-phthalate manometer. Inert gas then was added to give that total pressure which gave the desired percentage of Br_2. The

gases were allowed to stand and mix overnight. The mixture was fed into the evacuated tube through the opening near the membrane one or two minutes before the shock was run.

Extinction Coefficients of I_2

The light used was of two kinds. One was that from a 500 watt tungsten bulb operated at 120 volts and filtered through a combination of filters that gave the transmitted light curve shown in figure 9a. The other was that from a Hg arc filtered through a combination of filters that gave the transmitted light curve shown in figure 9b. Both curves were determined using a grating monochromator and the same photomultiplier used in the experiments. The filters used in 9a were a Bausch and Lomb 486 mμ interference filter and a Corning no. 3385 sharp cut filter. The filters used in 9b were a Bausch and Lomb 436 mμ interference filter and a Corning no. 3389 sharp cut filter. The tungsten lamp arrangement essentially gave light with a wavelength of 487 mμ. The Hg arc gave a wavelength of 436 mμ.

The room temperature extinction coefficient for the tungsten lamp arrangement was determined from very strong shock waves in I_2 mixtures. If the shock wave was so strong that all the I_2 dissociated then the change in photocurrent observed was that due to the initial absorption by the I_2. These experiments gave a value of 450 ± 20 for ϵ. The extinction coefficient ϵ is defined by $\log (I/I_0) = -\epsilon cl$, where I and I_0 are the transmitted and incident light respectively, c is the concentration in moles per liter of the absorbing

Figure 9 Light Used to Detect I_2

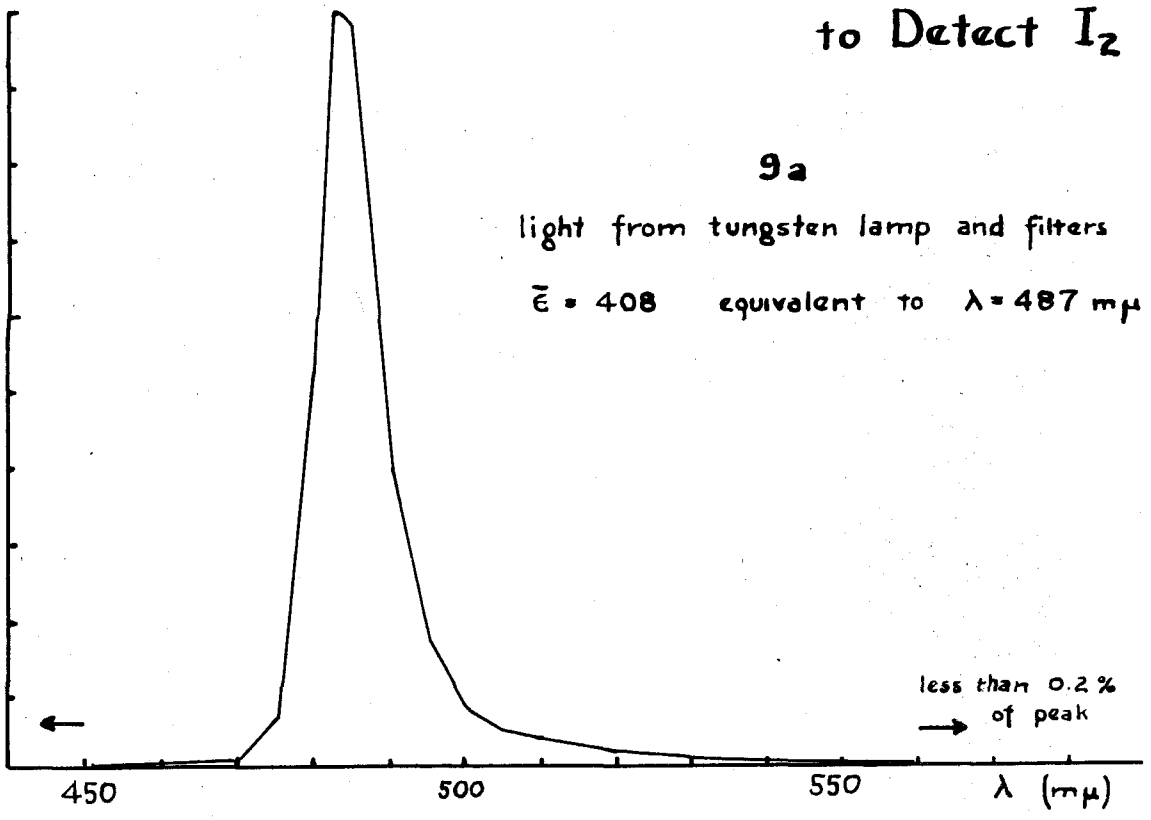

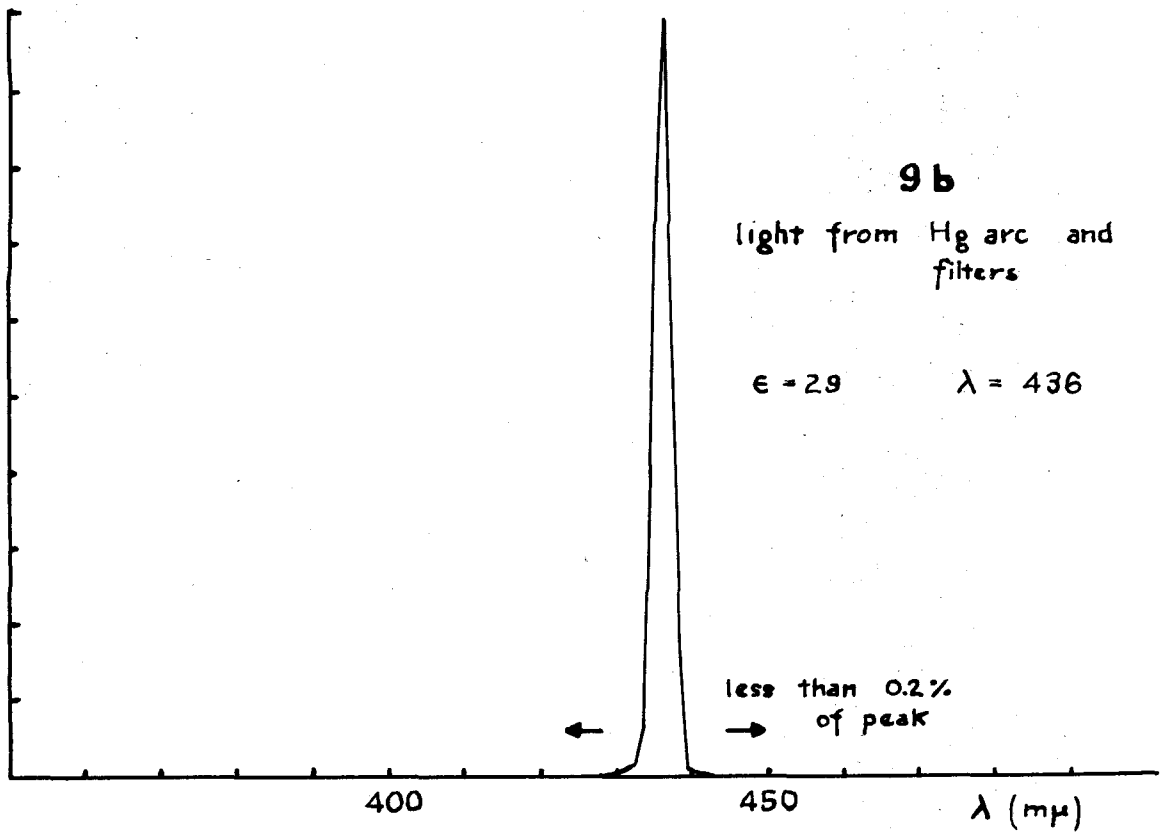

species, and l is the path length in centimeters. Combining the light transmission curves for the filters and light with the measured extinction coefficients of I_2 (4) the value $\epsilon = 408$ was found for the tungsten light arrangement. This value was believed to be the more accurate one and was used for calculations.

For the Hg arc (436 mμ) the room temperature extinction coefficient was taken as 29 from the measured values indicated (4).

From the measured velocity of the shock wave and a knowledge of the initial conditions the extinction coefficient of I_2 just behind the shock front can be calculated for every shock, whether or not there is a subsequent reaction. These calculations are outlined in Appendix C.

Figure 10 shows ϵ versus T for shocks in N_2-I_2 mixtures, where N_2 is assumed to be unrelaxed vibrationally. Figure 11 shows the same for N_2 assumed to be relaxed. Figure 12 shows the results from experiments in CO_2-I_2 mixtures assuming both relaxed and unrelaxed CO_2.

Curves were drawn through the experimental extinction coefficient points by eye. All the curves so obtained are shown together on figure 13. Relaxed and unrelaxed N_2 and CO_2 are compared with A, He, and relaxed and unrelaxed O_2, these latter through the courtesy of G. Schott (5). The N_2 and A were measured at both 487 mμ and 436 mμ, the CO_2 only at 487 mμ. Because some filters were changed in an attempt to increase the signal to noise ratio in the photomultiplier output

Figure 10 Extinction Coefficients of I_2 in N_2

N_2 assumed vibrationally unrelaxed

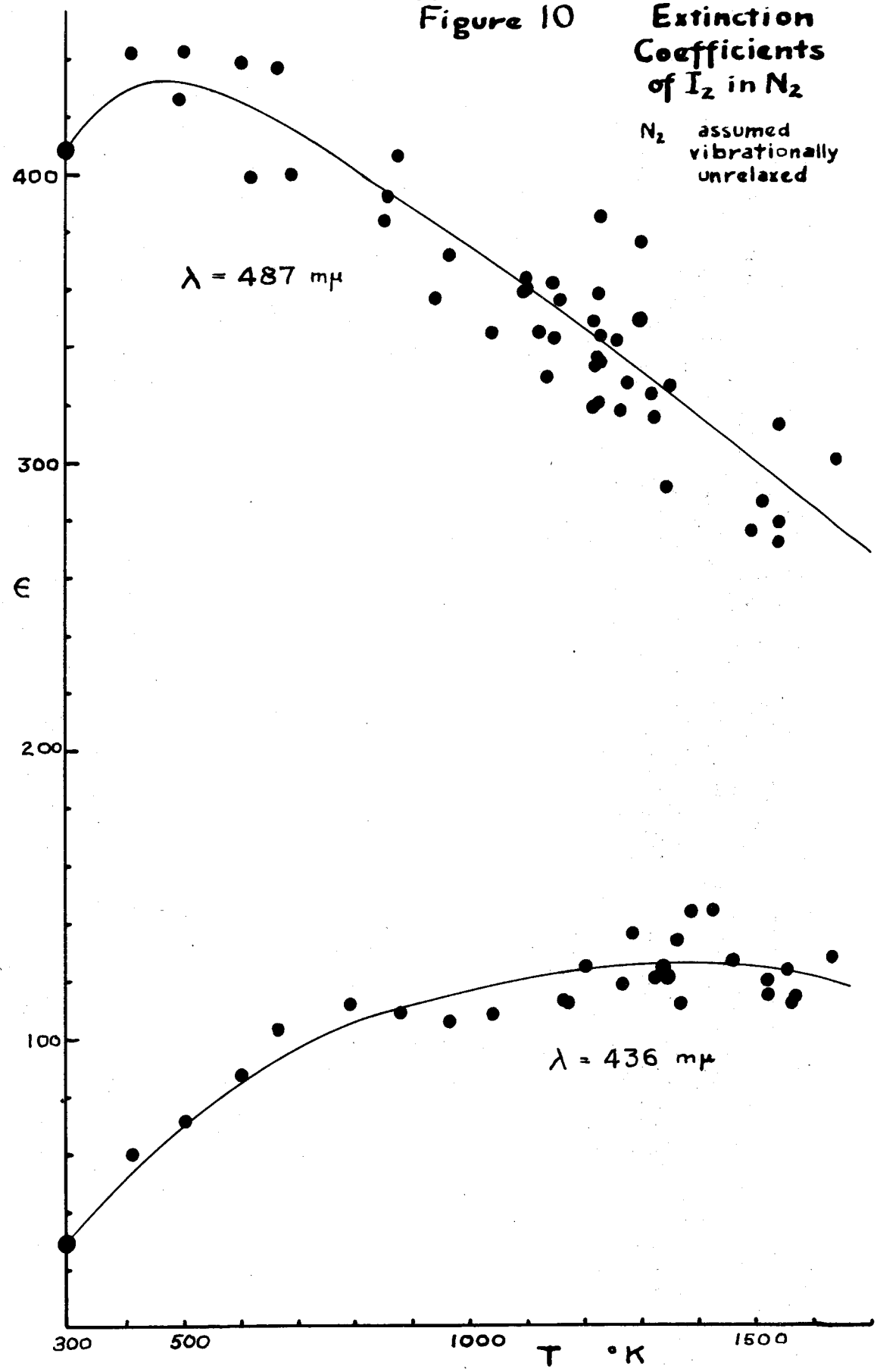

Figure 11 Extinction Coefficients of I_2 in N_2

N_2 assumed vibrationally relaxed

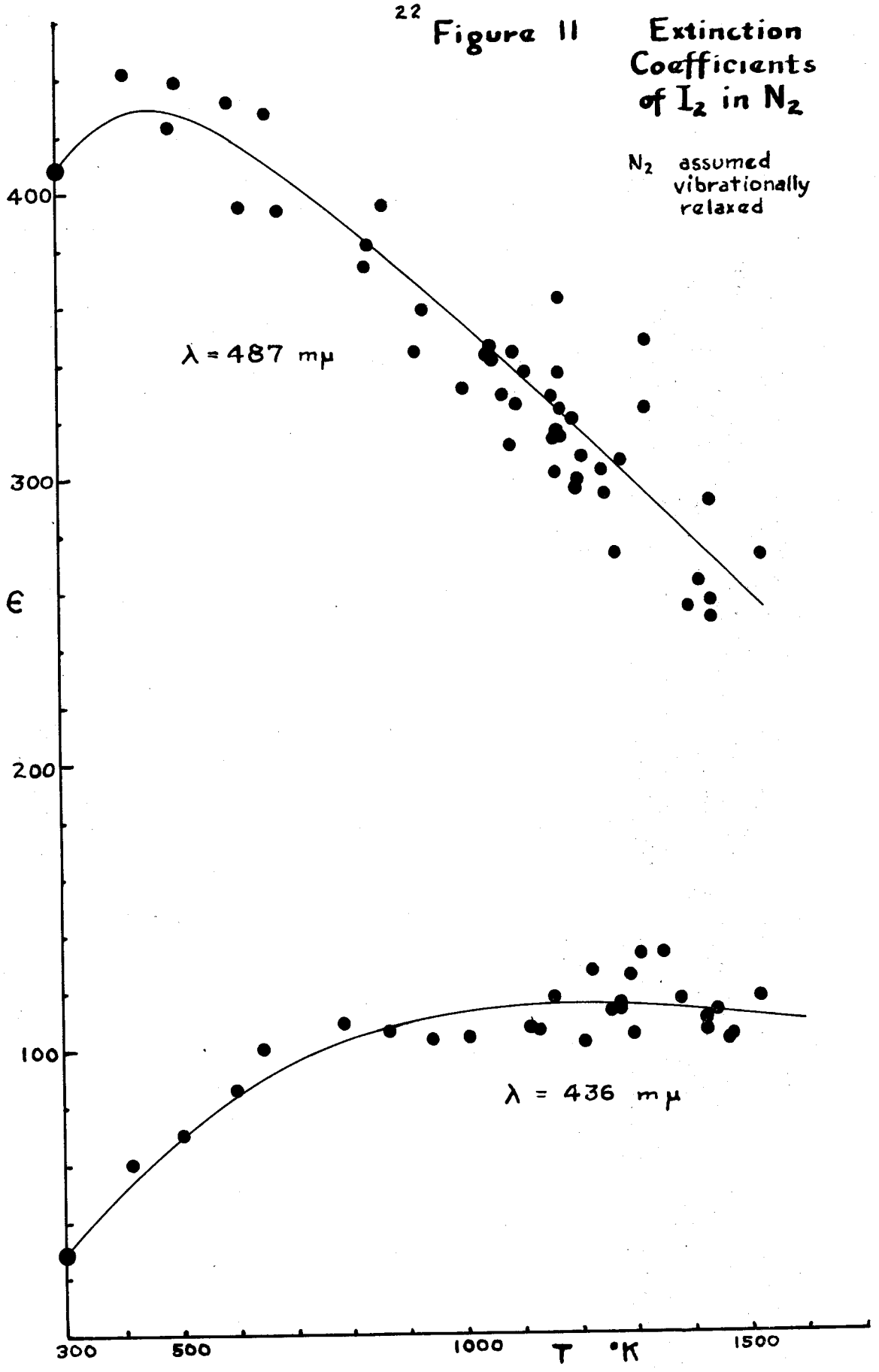

Figure 12 Extinction Coefficients of I_2 in CO_2

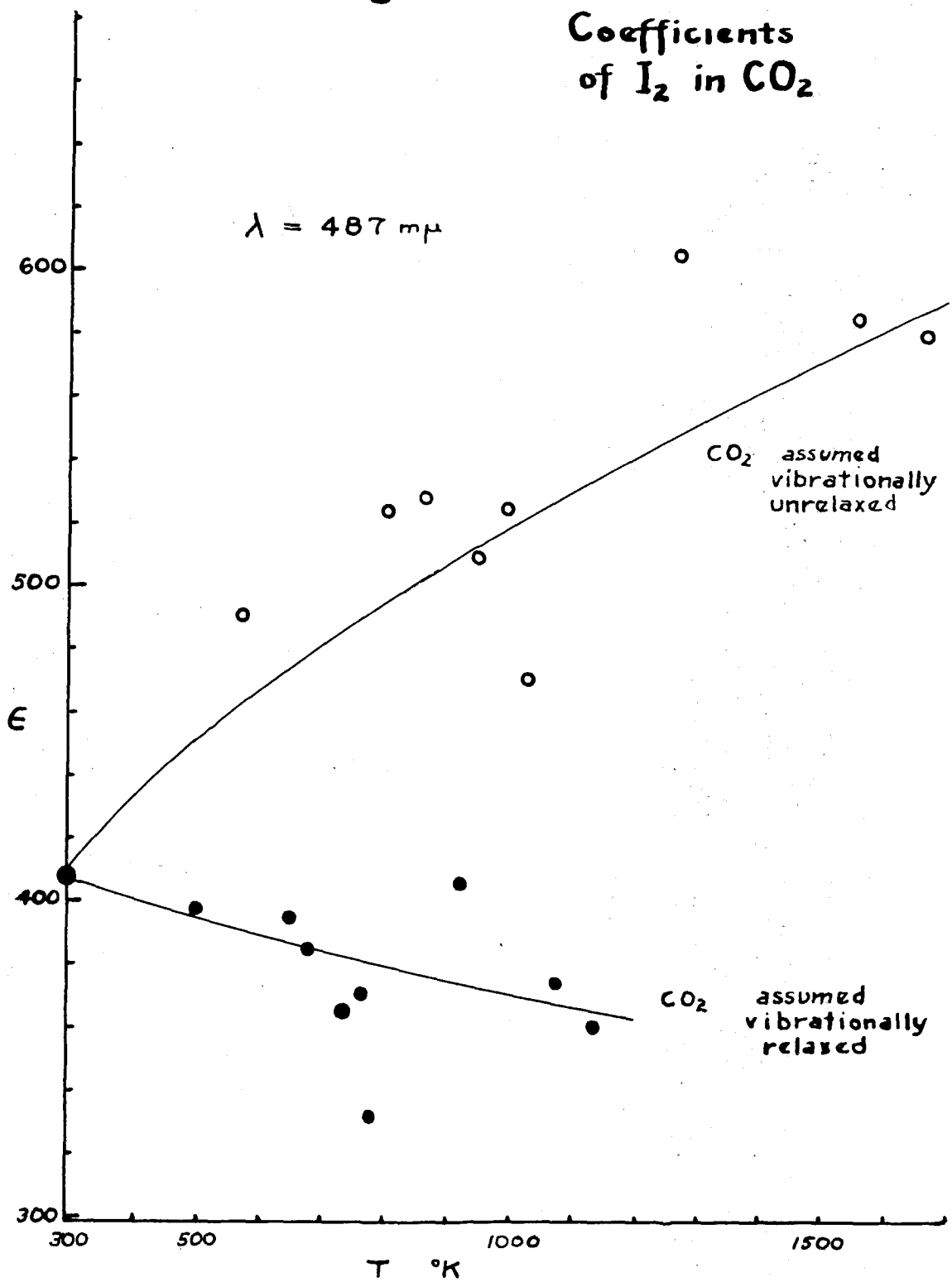

Figure 13 Extinction Coefficients of I_2 in various gases

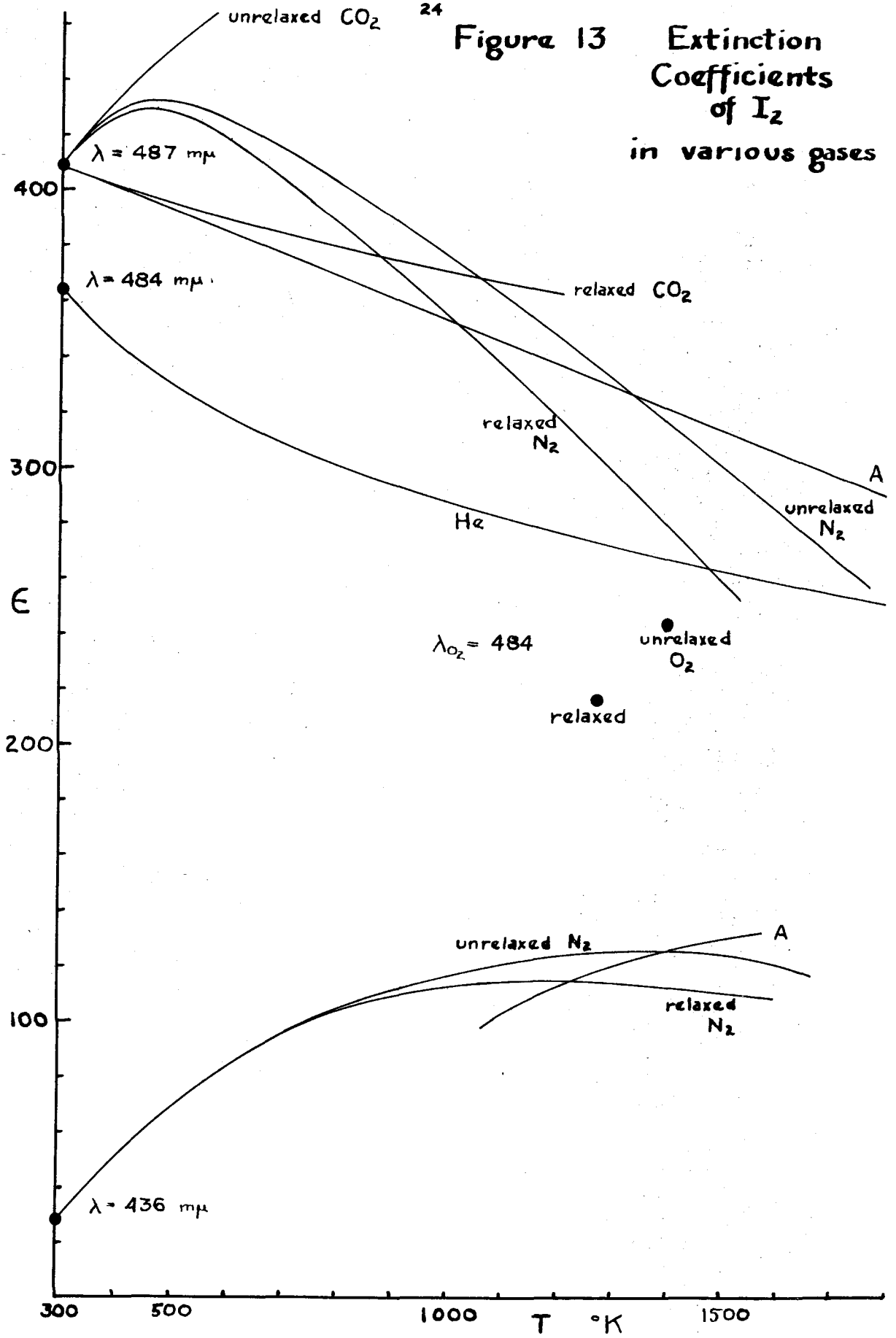

the He and O_2 were measured at what was effectively 484 mμ rather than 487 mμ.

On looking at the curves it is apparent that, except for CO_2, no decision can be made as to whether the gases with vibrational degrees of freedom are relaxed or unrelaxed. At 487 mμ the difference between the results in A and those in N_2, calculated assuming either relaxed or unrelaxed N_2, seems to be larger than experimental if one looks at the scatter of the experimental points. At 436 mμ the A and either N_2 agree within experimental error in the region from 1000°K to 1500°K where both were measured.

The comparison of the CO_2 curves with those of N_2 and A makes it seem clear that CO_2 is relaxed vibrationally. This is substantiated by the fact that the shock into CO_2 at the lowest temperature used seems to show a relaxation. This is shown in figure 6b, which should be contrasted with figure 6a, which is typical of the results in hotter CO_2 shocks. The relaxation of CO_2 has been measured in a shock tube using an interferometer to follow density changes (6). These measurements indicate that in all the CO_2 experiments the vibrational relaxation time would be a few microseconds or less, agreeing with the above conclusion that the CO_2 is relaxed. The relaxation time for CO_2 estimated in the one case where it was observed in the I_2 experiments agreed fairly well with that calculated from the reported results from the interferometer method.

The O_2 results when compared with the He results would

seem to show that the O_2 is vibrationally unexcited, but the differences are not enough to be sure of this. The rate constants measured for O_2 as the third body seem to indicate that the O_2 is relaxed, and this is probably the more conclusive evidence.

Allowing for the change in wavelength, the He and A results agree fairly well, although the scatter in the points for He is quite large. The experiments in He were more uncertain than the others due to non-uniform conditions behind the shock wave, probably due to cooling to the walls (5).

That the extinction coefficient of a colored gas, when measured in the continuous region of the spectrum, should change with the addition of a foreign gas is not expected. However the phenomenon is known in the case of Br_2 and it should not seem unreasonable here to find a small effect. The difference between the values measured in A and those measured in N_2 in these experiments are nevertheless so large at low temperatures as to suggest that there is some systematic error in the shock wave measurements. Careful static measurements of the extinction coefficient of I_2 at and near room temperature, that is, 300 to 400°K, in various inert gases would be interesting to decide this point. If the difference between A and N_2 as foreign gases is really as great as the results of the shock tube experiments indicate it should be readily measurable.

Extinction Coefficients of Br_2

In the experiments with Br_2 several different combina-

tions of lights and filters were used. Two were the same combinations used with I_2 and shown in figure 9. A third was the Hg arc with a Corning no. 5543 wide band pass filter and a Corning no. 3060 sharp cut filter. This combination let through the 436 mμ Hg line and some of the 406 mμ Hg line, as is shown in figure 14a. A fourth combination, shown in figure 14b, was the tungsten light with a Corning 436 mμ interference filter and a Corning no. 3060 sharp cut filter.

The extinction coefficient of pure Br_2 vapor has been measured as a function of wavelength (7), and, using these measurements, one can assign extinction coefficients to the light combinations shown. In the experiments with Br_2 it was possible to measure the extinction coefficient approximately in each experiment. This was because the tube was filled in about a minute and the change in photocurrent could be measured with some confidence since the drift rate of the photomultipliers was low. The results of these measurements are given in table 1. It should be noted that the Br_2 concentration is approximately the same in every experiment, so that the higher the percentage of Br_2 the lower the total concentration of all gases. The results in table 1 would then indicate that a pressure effect is very likely present.

That the extinction coefficient of Br_2 is affected by the presence of foreign gas, even in the continuum, is a known phenomenon (8). No measurements appear to have been made in argon but measurements in all other gases studied showed an increase in the extinction coefficient with increasing amount

Figure 14 Light Used to Detect Br_2

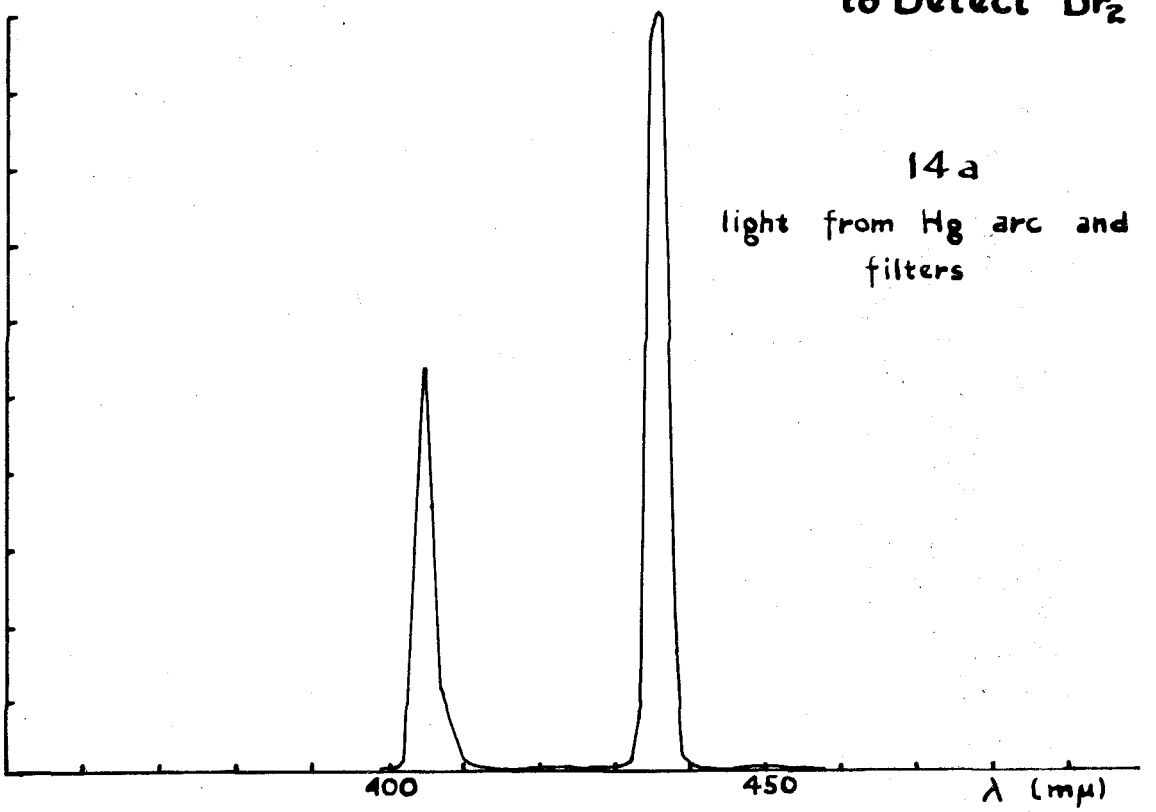

14 a

light from Hg arc and filters

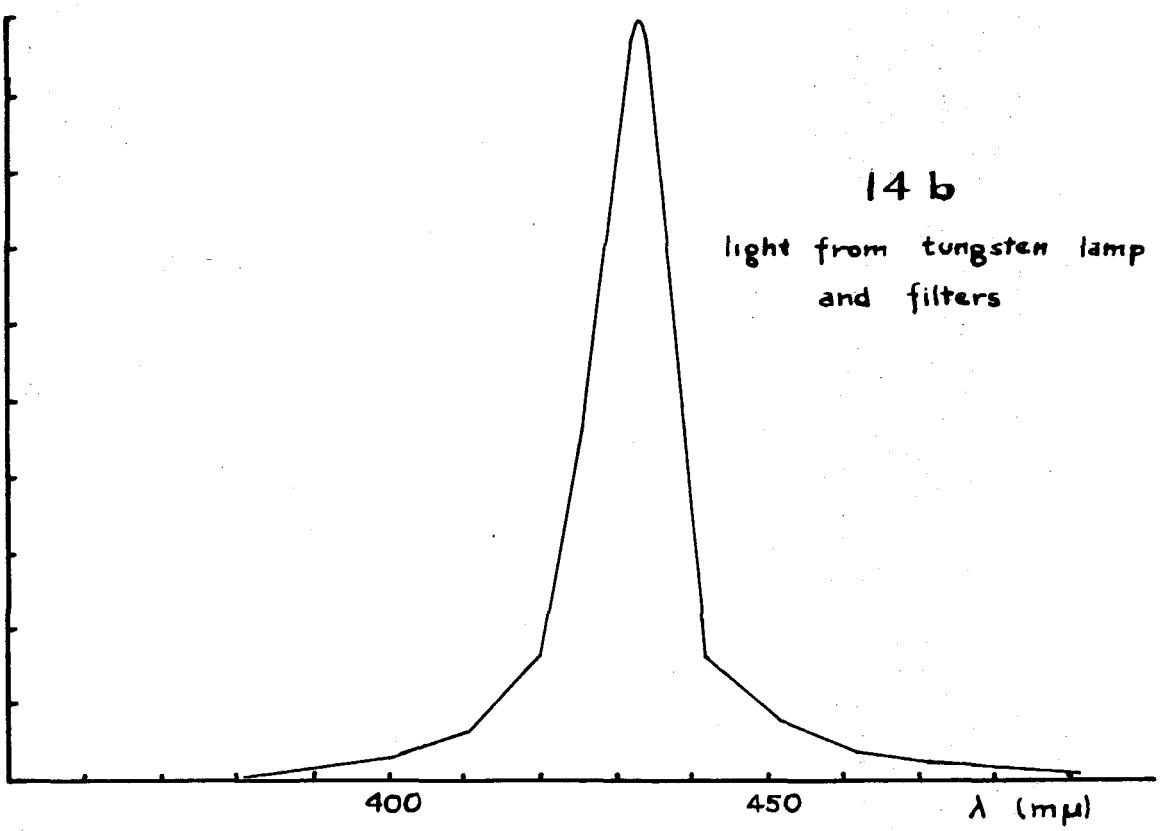

14 b

light from tungsten lamp and filters

Table 1

Room Temperature Extinction Coefficients of Br_2

light shown in figure	9a	9b	14a	14b
wave length (approx)	436 mμ	487	436 + 406	435
ϵ in pure Br_2 from reference 7	134	89	138	135

% Br_2 in mixture	ϵ				no. of runs	typical conc. moles/l.
1			154 ± 12	156 ± 13	11	2.6×10^{-3}
2	153 ± 9	105 ± 9			8	3.0
4	146 ± 5	121 ± 11			9	1.6
6	158 ± 2	90 ± 4			5	1.0
10			147 ± 6	153 ± 5	21	0.42
50			137 ± 7	144 ± 9	6	0.08
100			133 ± 5	133 ± 5	3	0.04

of foreign gas. This is what is found here. A few measurements were made in a Cary Recording Spactrophotometer of the extinction coefficient of Br_2 in 10% Br_2 - 90% A mixtures at various total pressures. In these experiments the extinction coefficient of Br_2 was found to fall with increasing concentration. This was an unsatisfactory point at which to leave this question, but since the measurement of extinction coefficients was not the primary purpose of these experiments no further work was done. It is clear that this is a problem in which more experimental data would be welcome.

It was decided to use the measured set of extinction coefficients in the calculations. At low fractions of Br_2 in the mixtures it does not matter much which extinction coefficients were used, but at higher fractions it can make a great difference in the rate constant. This will be gone into more fully in the section on kinetics.

The measured values of the extinction coefficients of Br_2 are shown in figures 15 and 16. For comparison, values determined up to 900°K (7) in a conventional manner for pure Br_2 are shown also. The temperature dependence found here agrees with this earlier work as well as can be expected in view of the fact that pressure effects have shifted the values of the extinction coefficients.

The Dissociation Reactions

The dissociation of diatomic molecules into atoms requires that some otherwise non-reacting atom or molecule collide with the diatomic molecule and transfer sufficient

Figure 15 Extinction Coefficients of Br_2

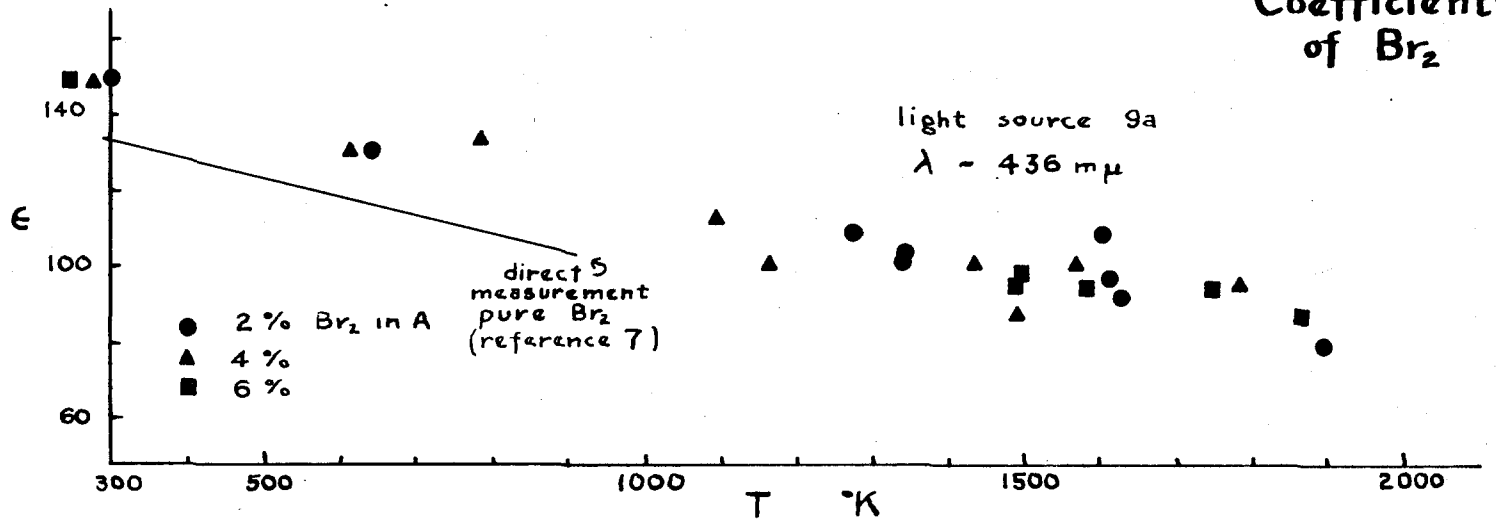

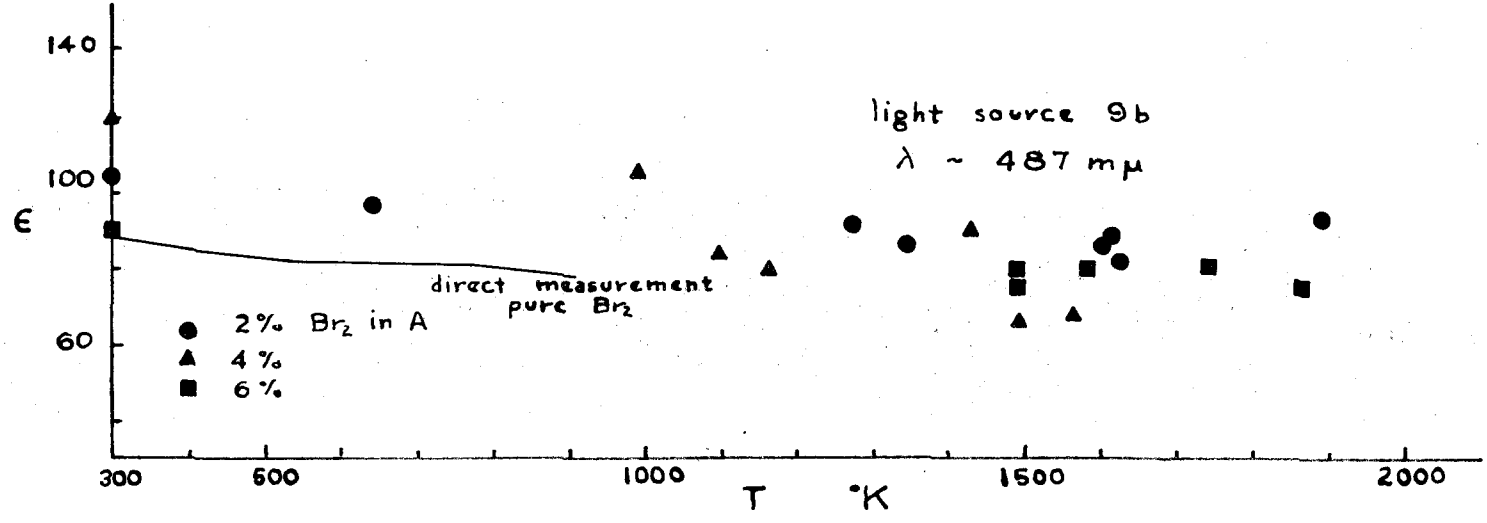

Figure 16 Extinction Coefficients of Br_2

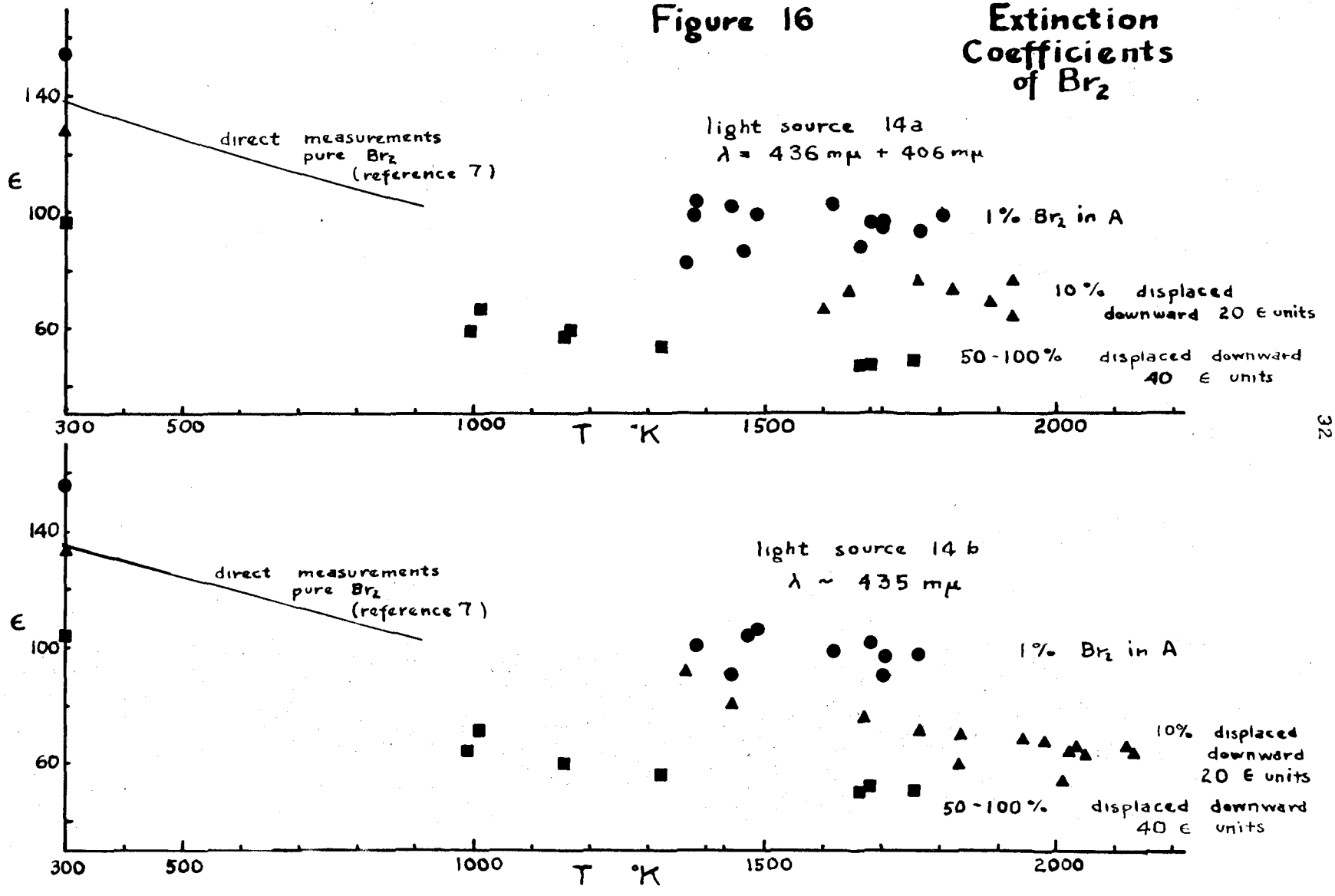

energy to it to allow it to dissociate. The equation describing this reaction is

$$M + X_2 \longrightarrow M + X + X \quad ,$$

where M is the atom or molecule with sufficient energy to dissociate the X_2 molecule. The recombination of the two atoms into a molecule is described by the reverse of the reaction above

$$M + X + X \longrightarrow M + X_2 \quad .$$

In this reaction M has the role of taking off the excess energy liberated in the recombination. In this reaction M is called the third body, and in the following pages it will be referred to as such whether recombination or dissociation is being considered.

The kinetics of the dissociation and recombination can be described by the equation

$$\frac{d(X_2)}{dt} = - k_D(X_2)(M) + k_R(X)^2(M) \quad ,$$

where (M) represents the total concentration of third bodies. (All concentrations will be given in moles per liter and all times in seconds.) The two rate constants k_R and k_D are related by $k_D = k_R K$, where K is the equilibrium constant for the reaction

$$X_2 \rightleftharpoons 2X \quad .$$

Kinetics of I_2 Dissociation

On fifty-one oscilloscope traces taken of forty shock waves it was possible to measure the rate of dissociation of I_2 in the presence of N_2. These covered a temperature range

from 1100 to 1740°K if the N_2 is assumed unrelaxed, or from 1060 to 1610°K if the N_2 is assumed relaxed. The total concentrations of gas used varied from about 0.4×10^{-3} to 2.0×10^{-3} moles per liter, and the I_2 percentage varied from about 0.4 to 2 percent. Rate constants were calculated either by using an integrated rate expression or by measuring the initial slope of the trace, both as explained in Appendix D. The results were substantially the same by either method of calculation.

The rate constants so measured were converted to rate constants for recombination, k_R. The values of k_R obtained are plotted in figures 17 and 18 as log k_R versus log T. They could just as well have been plotted as log k_R versus 1/T. The points are so scattered that which of these two forms gives the better straight line could not be determined. Figure 17 shows the points assuming the N_2 to be unrelaxed, figure 18 assuming it to be relaxed. The straight lines drawn on the two figures were fitted by least squares to the points shown. The points were weighted depending on the smoothness of the curves, the value of the extinction coefficient found, that is, how well the extinction coefficient agreed with that obtained from an average of all the data, and similiar considerations.

The equations for these straight lines are

$$\log k_R = 8.833 - 1.651\ (\pm 0.242)\ \log(T/1000)$$

$$\log k_R = 9.007 - 1.376\ (\pm 0.267)\ \log(T/1000)$$

for unrelaxed and relaxed N_2 respectively. The errors given

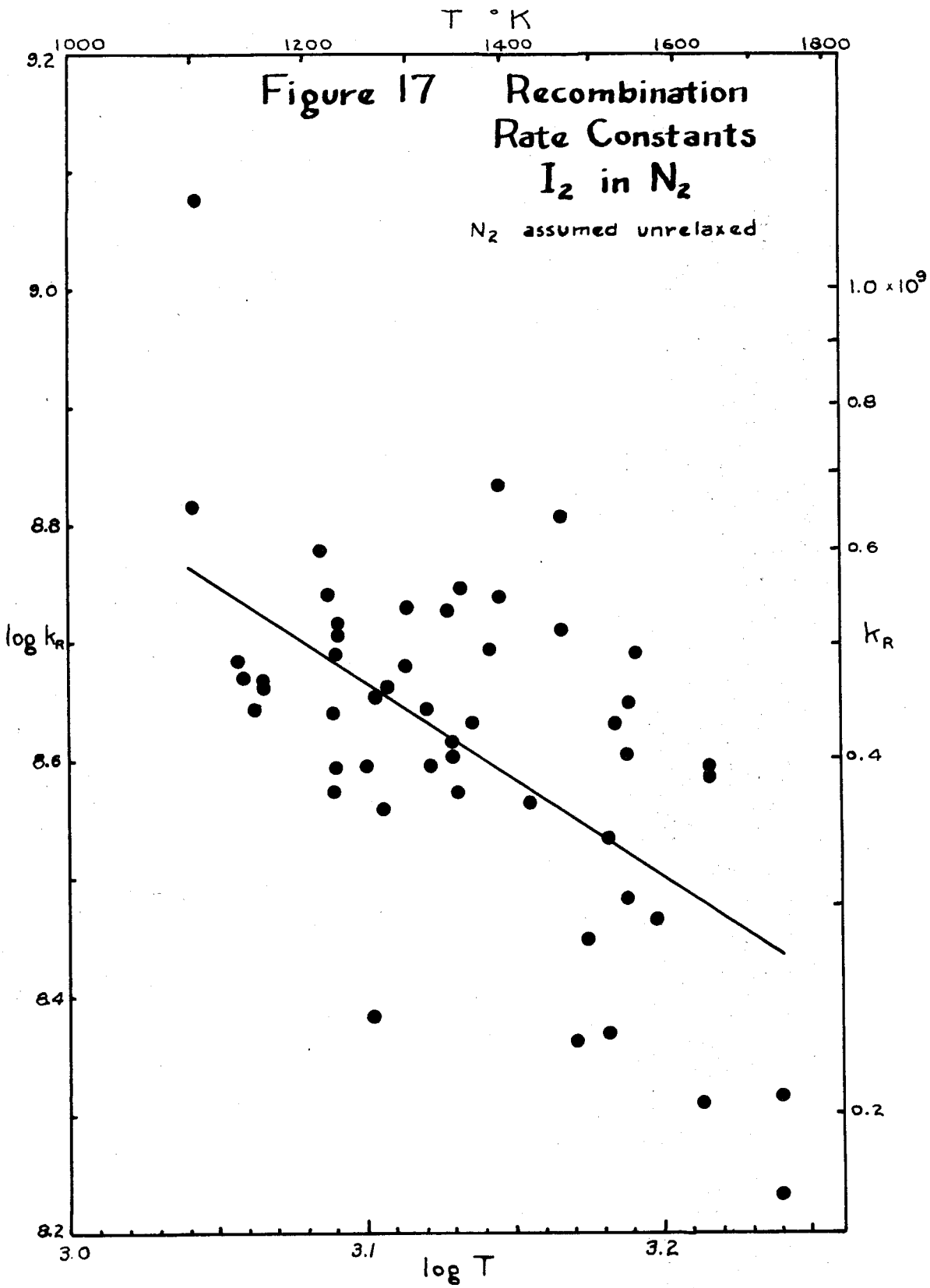

Figure 17 Recombination Rate Constants I_2 in N_2

N_2 assumed unrelaxed

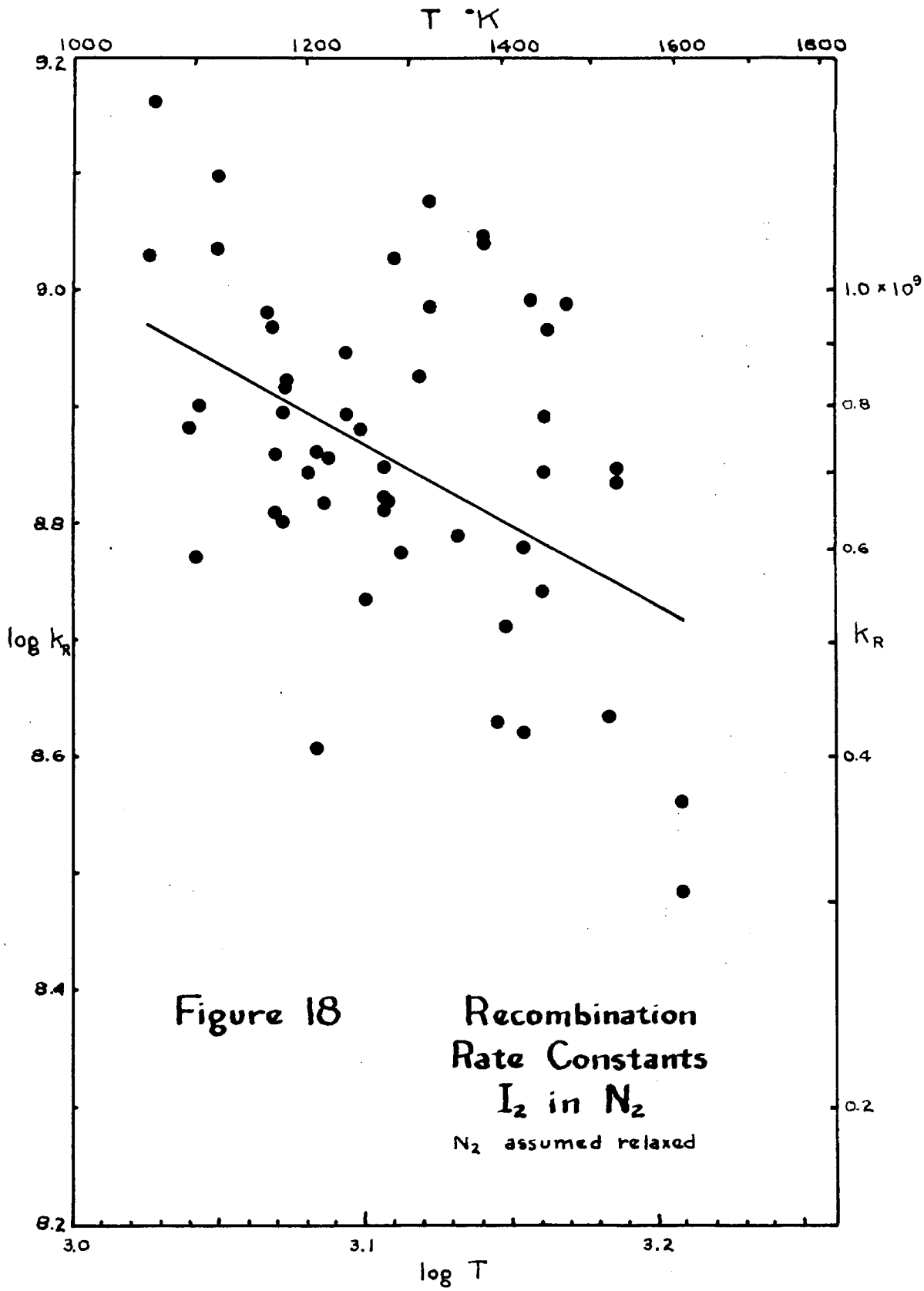

Figure 18 Recombination Rate Constants I_2 in N_2

N_2 assumed relaxed

are probable errors, calculated according to Margenau and Murphy (9). The probable errors in log k_R at the centers of the range covered are 0.012 (T = 1344) and 0.013 (T = 1274) respectively.

The corresponding equations for log k_R versus 1/T are

$$\log k_R = 7.732 + 1053\ (\pm 449)/T \qquad \text{and}$$

$$\log k_R = 8.138 + 925\ (\pm 543)/T$$

for unrelaxed and relaxed N_2 respectively. The probable errors in log k_R at the centers of the range covered are 0.004 (T = 1335) and 0.005 (T = 1267) respectively. If one converts the slopes in this formulation to energy units one finds 4.81 ± 2.05 and 4.23 ± 2.48 kilocalories per mole respectively.

In CO_2 only two experiments yielded rate constants. These were the following:

T = 1077	$k_R = 1.85 \times 10^9$	
1137	1.30	CO_2 assumed relaxed,
1559	2.85×10^6	
1666	2.50	CO_2 assumed unrelaxed.

Looking at these and comparing them with the N_2 results which are of the order of 10^9 it appears clear that CO_2 is relaxed, in agreement with the conclusion from extinction coefficients.

The rate of recombination of I atoms into molecules in various inert gases has been measured at room temperature by a flash photolysis technique by a number of experimenters (10, 11, 12, 13, 14). Although recent work indicates that the older values for rate constants are too high only one of the earlier reports gives rate constants for the gases studied here. Accordingly this work (12) is used for comparison.

The high temperature results for the I_2 dissociation in N_2 and CO_2 have been described. Other work in this laboratory has yielded similar results for A, O_2, and He (5). These results are all collected in figures 19 and 20. These show 293°K (room temperature) and 400°K results from flash photolysis, and the high temperature shock wave results. Figure 19 combines these on a plot of log k_R versus log T. Figure 20 shows log k_R versus 1/T. Since the slopes of the results at high temperatures are all quite uncertain only a single point is used to represent each set of shock wave results for a particular inert gas.

From these two figures it appears that plotting log k_R versus 1/T seems to fit the data over the entire measured range better. If one accepts this as the correct representation then it would appear very likely that N_2 is vibrationally unrelaxed at high temperatures. The previous conclusion that CO_2 is relaxed is supported. No decision can be made for O_2, but judging from the slopes of the other lines relaxed O_2 is possibly more likely. Although the He results give a good straight line it should be remembered that there was some uncertainty as to the correctness of the high temperature points.

Recent flash photolysis results (14, 15) have indicated that I_2 molecules are themselves exceptionally efficient as third bodies. One result (14) gives I_2 as 285 times more efficient than A. An attempt was made to determine this ratio at high temperatures by plotting the percent deviation of k_R from the smoothed curve values against the percent I_2 for each

Figure 19 I_2 Recombination Rate Constants

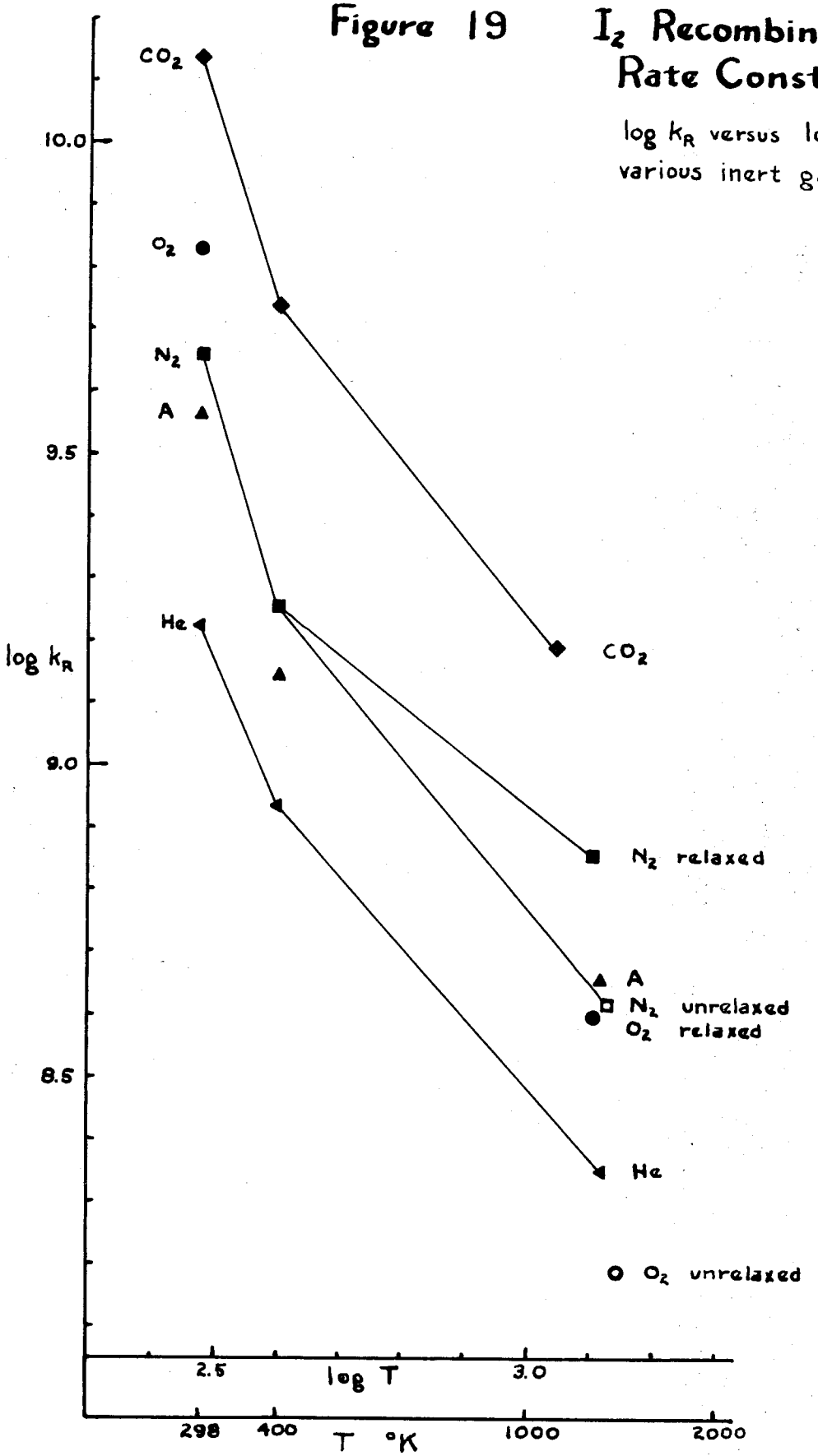

Figure 20 I_2 Recombination Rate Constants

$\log k_R$ versus $\frac{1}{T}$
various inert gases

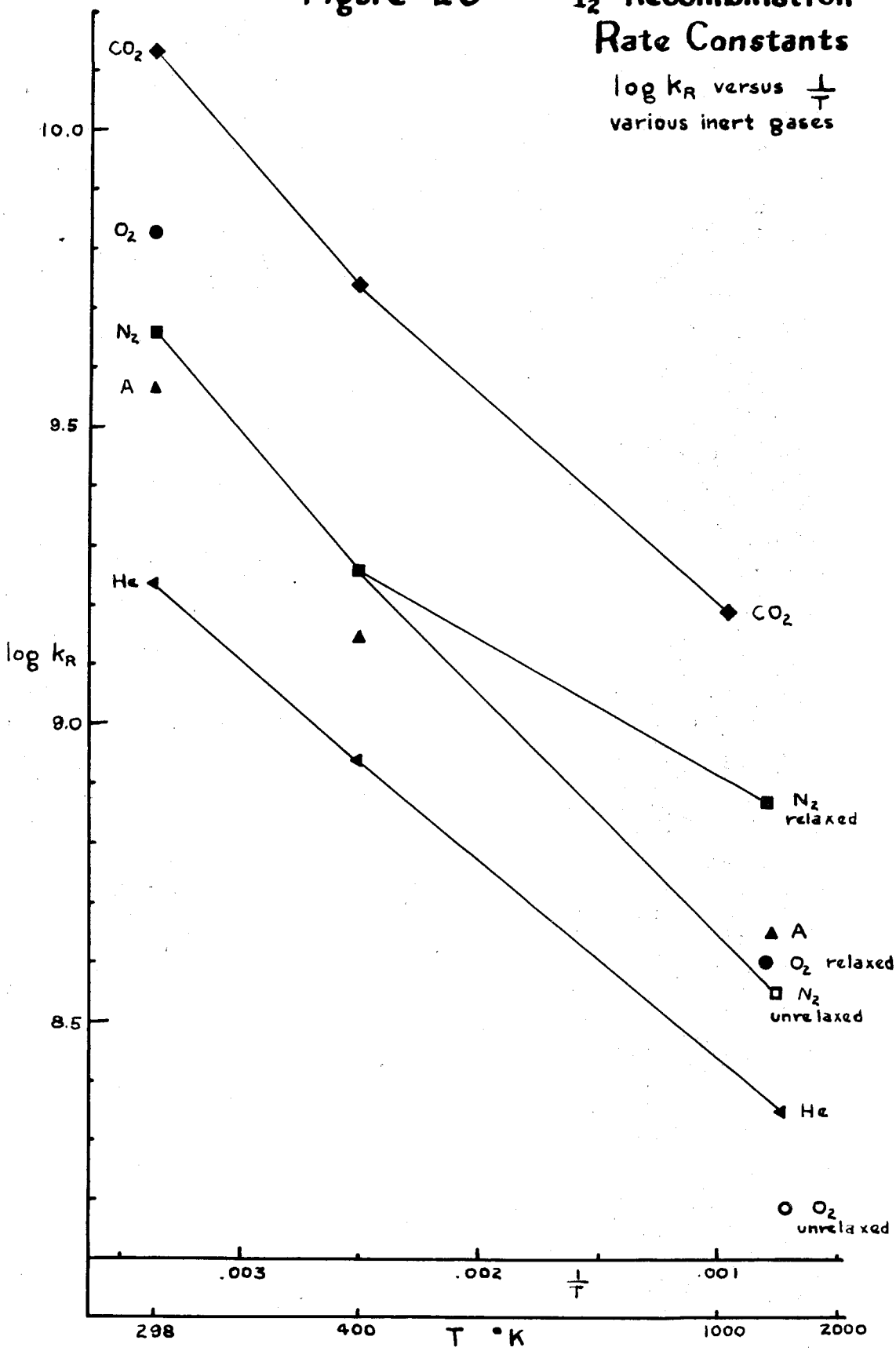

shock. Ideally this would give a straight line, the slope of which would be the ratio. Actually the scatter of the results was so great that no reliable value could be measured. That the ratio is probably between 0 and 30 is all that could be concluded. Similiar attempts to measure this ratio in A led to the conclusion that I_2 is less than 25 times as efficient as A (5).

Kinetics of Br_2 Dissociation

On sixty-two oscilloscope traces from forty-two shocks it was possible to measure the rate of dissociation of Br_2 in A. The percentage of Br_2 varied from one to ten. The one percent Br_2 results are the only ones that are regarded as very reliable since the correction terms become quite large and uncertain as the percentage of Br_2 increases. The results in one percent Br_2 were obtained over a temperature range from 1380 to 1771°K. These are shown, along with a straight line fitted through them by least squares in figure 21. Also shown in figure 21 are the results from two, four, six, and ten percent mixtures. The total concentration of gas before the shock was of the order of 2.8×10^{-3} moles per liter in the one percent mixtures and proportionately less with the larger percentages of Br_2.

The larger percentages of Br_2 were used in an effort to measure the rate constant for Br_2 as the third body. However, as is shown in Appendix D, the rate constants depend quite markedly on the value of $d\epsilon/dT$, which from figure 16 can be seen to be uncertain by a factor of two at least. Because of

Figure 21

Recombination Rate Constants Br_2 in A

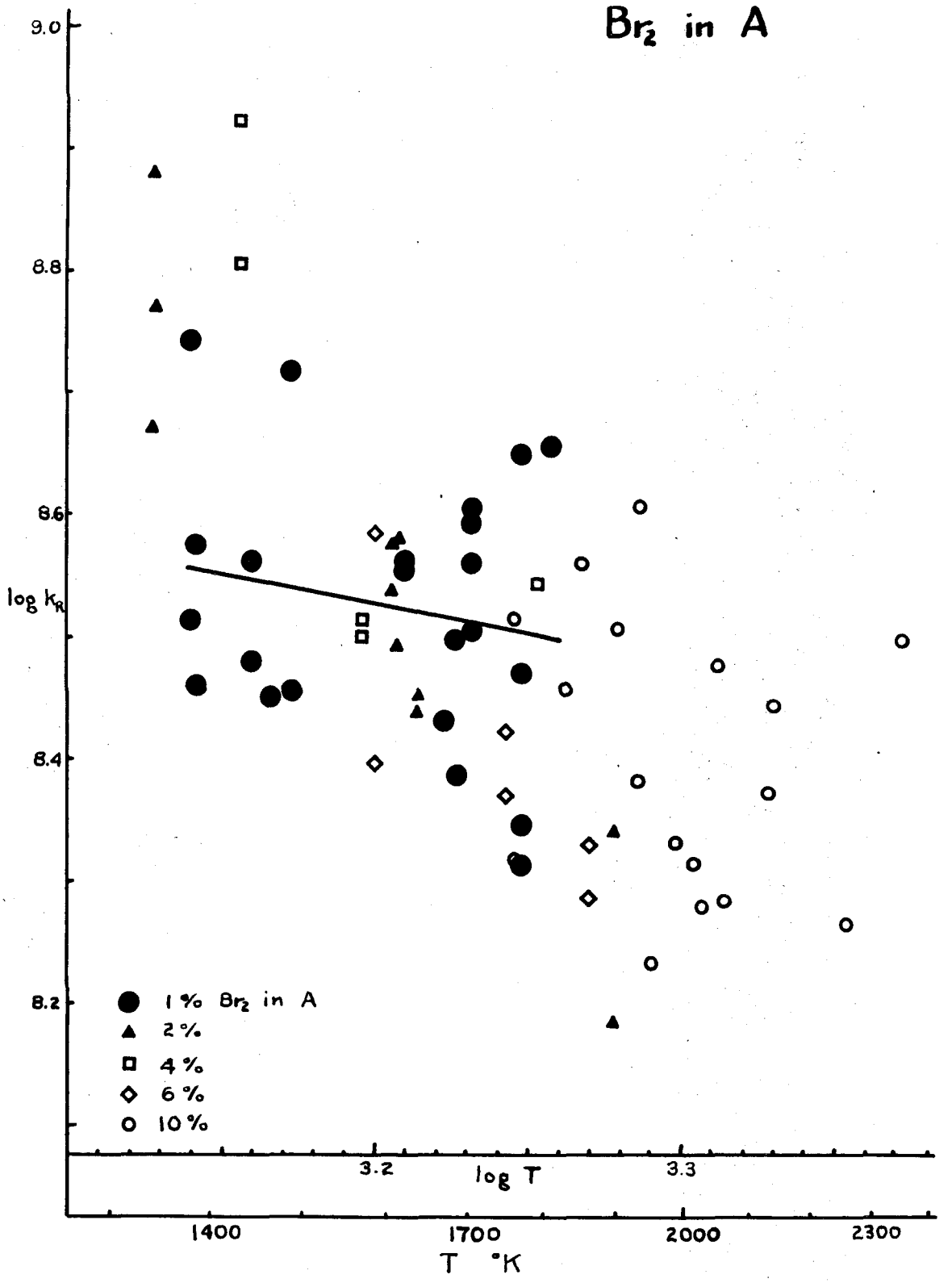

this, in the ten percent Br_2 experiments the rate constants were uncertain by a factor of about two. Considering all the data as in the case of I_2 it appears that Br_2 is between 0 and 8 times ~~more~~ as effective as a third body for the recombination. The only value given for this ratio at room temperature is >14 (16), and this is fairly uncertain.

A more accurate estimate of this ratio could probably be determined in the same manner as was attempted above except that CO_2 should be used as the inert gas. The heat capacity of CO_2 at high temperatures is over twice that of A so that the temperature change in a one percent Br_2 shock wave in CO_2 is less than half that in a one percent Br_2 shock in A. This makes the correction terms correspondingly less and therefore the uncertainty caused by the uncertainty in $d\epsilon/dT$ less important. Determination of the rate constant at one particular temperature in one percent and five percent Br_2 shocks should then allow the measurement of the relative efficiency of Br_2 and CO_2 as third bodies. It would also be better to observe the reaction with light around 487 mμ where $d\epsilon/dT$ is less than at 436 mμ.

Figure 22 shows the room temperature value (13) combined with the shock wave value on two plots. One is log k_R versus log T and the other log k_R versus 1/T. That the measured high temperature slope agrees better with the 1/T plot is probably meaningless. No intermediate point is available here to compare the two methods of plotting the results.

The high temperature results for Br_2 can be represented by the equations

Figure 22 Br_2 Recombination Rate Constants in argon

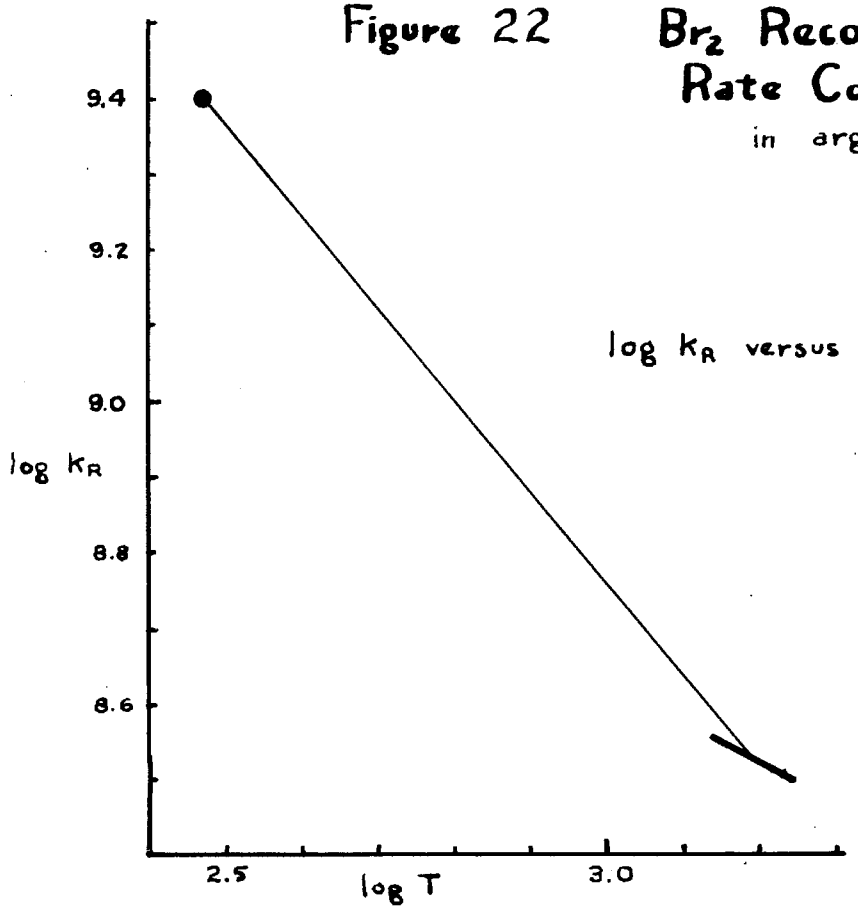

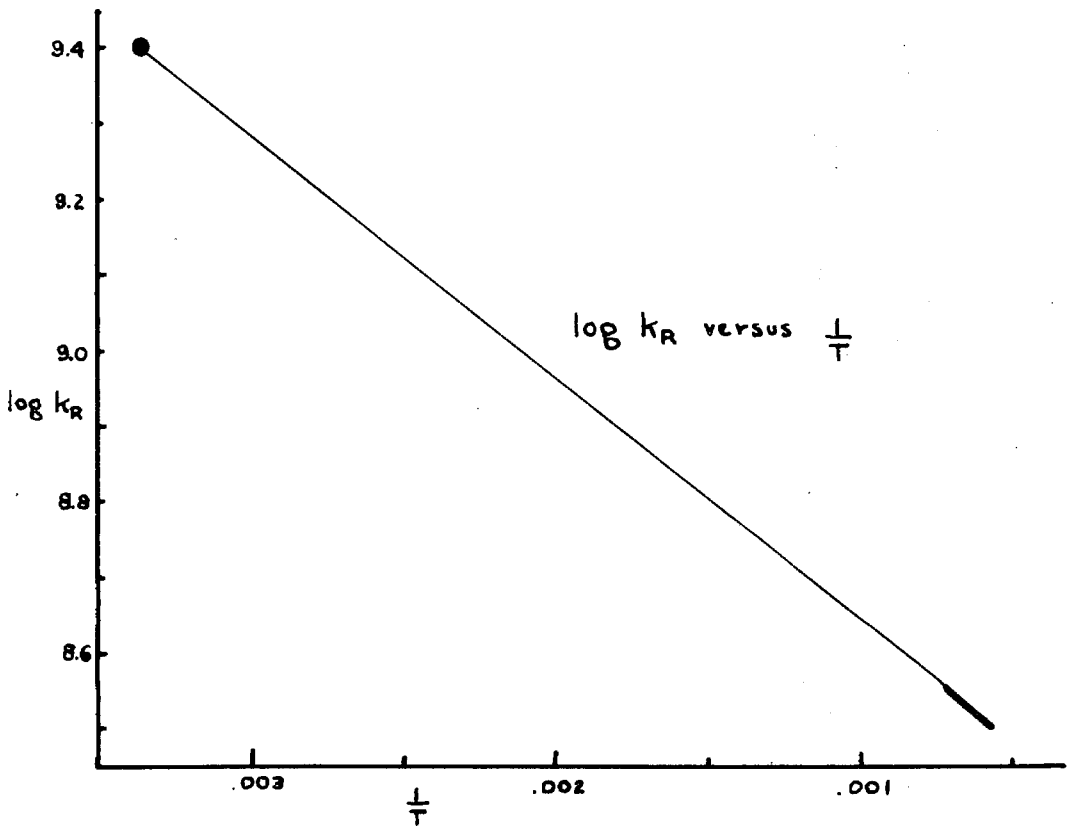

$$\log k_R = 8.631 - 0.524\ (\pm 1.187) \log 1000/T$$

or $$\log k_R = 8.300 + 357\ (\pm 803)/T \quad .$$

The probable errors in log k_R in the center of the range covered are 0.049 (T = 1595) and 0.049 (T = 1590) respectively. The latter slope is equivalent to an energy of 1.63 ± 3.67 kilocalories per mole.

Discussion

The experiments described here are a more stringent test of the shock tube in chemical kinetics than the N_2O_4 experiments previously described (1). They point up the advantages of the shock tube quite clearly but they also point up some serious deficiencies. The advantages are that very fast reactions can be studied, that high temperatures can be readily attained for kinetic measurements in a region where even static measurements are troublesome by ordinary means, and that one is more or less assured of a homogeneous reaction. The disadvantages are in some respects necessary consequences of the advantages. Because an essential assumption of the shock wave method is that in the short time available the walls do not interact with the shocked gas the reactions which are to be studied must be fast reactions. This limits the range of pressure and temperature over which a particular reaction can be studied. Also since the temperature of the walls is not directly related to the temperature of the gas the behavior of the gas is governed by purely hydrodynamical considerations and if any reaction takes place it does so in a highly non-isothermal medium. When working in temperature

ranges far above room temperature the need for essentially static data, such as extinction coefficients or equilibrium constants, to more accuracy than that attainable by the shock wave method, is often felt, and the data are found to be unavailable. At temperatures high enough the cooling effect of the walls does become important and limits still further the time in which observations can be made. Finally the electronic and photometric devices with which measurements are made are being used at their limits because the resolving times required are so small. Some of these problems are unavoidable. Some problems, like the electronic and photometric equipment, and the lack of high temperature static data can and will become less serious with time.

The results recorded here are interesting in that they confirm earlier conclusions that the rate of recombination of I atoms decreases with increasing temperature, and extend these earlier conclusions to considerably higher temperatures. Such behavior can be interpreted as meaning that the kinetic energies of two I atoms must be below the average kinetic energy at a particular temperature for recombination to take place. The question of how this temperature dependence should be described, as log k_R versus log T, or as log k_R versus 1/T, is an interesting one. If the 1/T description is correct, as the overall survey of the existing data would indicate, then it would appear that an energy is associated with the recombination. One is left with the pleasantest of speculations to account for this energy. Unfortunately shock

waves alone cannot give results precise enough to determine if this 1/T representation is right, at least not in the present, or in an immediately forseen future apparatus. The shock wave points do provide an extension to flash photolysis results which could and should be obtained up to about 800°K to decide this point.

Table 2 shows the equations obtained by combining the room temperature points with the high temperature points for both methods of expression. If the form $k_R = AT^{-n}$ is correct one might expect that n is the same for any third body. That n varies considerably is perhaps another argument for the form $k_R = A \exp(E/RT)$.

Comparison of the results for Br_2 and I_2 in A show that the recombination rates are about the same, and have about the same temperature dependence, even though the dissociation rates are quite different. It would be interesting and quite readily possible to measure the rate of dissociation and recombination of Cl_2. It would be interesting to measure the rate of dissociation and recombination of F_2.

In doing future work either with Br_2 and I_2 and other inert gases, or with Cl_2 and F_2 in any inert gases, it seems clear that it is not worth trying to cover a large range of temperature, but rather to do enough runs at one temperature to have some confidence in the average, and to cover a range of temperatures by combining shock tube and flash photolysis measurements.

Table 2

Recombination Rate Constants
between Room and High Temperature

Unrelaxed N_2-I_2		
k_R =	$4.34\times10^{9}(T/300)^{-1.73}$ or	$= 1.57\times10^{8}\exp(1.95/RT)$
Relaxed N_2-I_2	$4.41\times10^{9}(T/300)^{-1.23}$	$4.28\times10^{8}\exp(1.37/RT)$
Relaxed CO_2-I_2	$13.0\times10^{9}(T/300)^{-1.76}$	$6.37\times10^{9}\exp(1.78/RT)$
A-I_2	$3.52\times10^{9}(T/300)^{-1.40}$	$2.44\times10^{8}\exp(1.57/RT)$
He-I_2	$1.65\times10^{9}(T/300)^{-1.32}$	$1.28\times10^{8}\exp(1.51/RT)$
Relaxed O_2-I_2	$6.42\times10^{9}(T/300)^{-1.92}$	$1.71\times10^{8}\exp(2.14/RT)$
Unrelaxed O_2-I_2	$6.36\times10^{9}(T/300)^{-2.41}$	$5.71\times10^{8}\exp(2.78/RT)$
I_2-I_2		
between	$8.50\times10^{11}(T/300)^{-2.97}$	$2.78\times10^{9}\exp(3.36/RT)$
and	$8.05\times10^{11}(T/300)^{-5.21}$	$3.50\times10^{7}\exp(5.90/RT)$
A-Br_2	$2.5\times10^{9}(T/300)^{-1.19}$	$2.14\times10^{8}\exp(1.45/RT)$

Appendix A

Definition of symbols

a velocity of sound $= \left[\frac{\gamma RT}{W}\right]^{1/2}$ in cm/msec where given numerically

A concentration of atoms of dissociating gas moles/liter

α degree of dissociation

B bursting pressure ratio $= \frac{P_3}{P_1}$

β enthalpy function $= 2\mathcal{H} - 1$

c total concentration (formal) moles/liter

D density

δ a specific variation in some parameter with respect to ϕ, for example $\delta\Pi = \Pi_{\phi=0.01} - \Pi_{\phi=0}$

Δ shock density ratio $= \frac{D_2}{D_1}$

E specific internal energy

E° molar internal energy

ϵ molar extinction coefficient (decadic) liter/mole cm

ϕ mole fraction of reacting gas referred to no dissociation

γ heat capacity ratio $= \frac{C_p}{C_v}$

H specific enthalpy

H° molar enthalpy

H_o° molar enthalpy at absolute zero

i light intensity

i_o incident light intensity

I concentration of inert gas — moles/liter

k specific reaction rate — concentrations in moles/liter times in seconds

K equilibrium constant $= \frac{R^2}{M}$ — moles/liter

K_P equilibrium constant $= \frac{P_A}{(P_M)^{1/2}}$ — $(\text{atmospheres})^{\frac{1}{2}}$

$\varkappa$ (kappa) dimensionless molar enthalpy function $= \frac{H^\circ - H_o^\circ}{RT}$

l length of light path

$\ln$ natural logarithm

$\log$ base 10 logarithm

M concentration of molecules of dissociating gas — moles/liter

P pressure

Π shock pressure ratio $= \frac{P_2}{P_1}$

R gas constant — in whatever units are convenient

s shock velocity — in cm/msec where given numerically

t time

T temperature

τ apparent time in shock wave

Θ shock temperature ratio $= \frac{T_2}{T_1}$

u velocity of gas relative to shock front

U_d molar heat of dissociation (one mole of molecules)

U_i molar heat of ionization (one mole of atoms)

v cold front velocity in cm/msec where given numerically

V specific volume

W molecular weight

$\overline{W_\alpha}$ mean molecular weight for α dissociation

$\overline{W}$ mean molecular weight $\alpha = 0$

Subscripts

$_o$ initial value that is at t or $\tau = 0$

$_\infty$ equilibrium value that is at t or $\tau = \infty$

$_1$ refers to conditions before the shock wave

$_2$ refers to conditions behind the shock wave

$_3$ refers to conditions in the undisturbed driving gas

$_\phi$ refers to values at a particular ϕ

$_A$ refers to atoms (if on k refers to atoms as third body)

$_M$ refers to molecules (if on k molecules as third body)

$_I$ refers to inert gas (if on k inert gas as third body)

$_D$ on k refers to dissociation

$_R$ on k refers to recombination

Appendix B

Shock Wave Equations

The equations to be used for shock waves in which dissociation or ionization occur will be developed. The development will be based on a stationary shock wave in a tube of uniform area. The transformation to a shock wave moving into a gas which is stationary in the laboratory system is straightforward, and involves only the two relations $u_1 = s$ and $u_2 = s - v$.

For a stationary shock wave the following equations hold:

(1) $D_1 u_1 = D_2 u_2$ conservation of mass

(2) $P_1 + D_1 u_1^2 = P_2 + D_2 u_2^2$ conservation of momentum

(3a) $E_1 + \frac{P_1}{D_1} + \frac{u_1^2}{2} = E_2 + \frac{P_2}{D_2} + \frac{u_2^2}{2}$ conservation of energy

(3b) $H_1 + \frac{u_1^2}{2} = H_2 + \frac{u_2^2}{2}$

From these one obtains

(4a) $H_2 - H_1 = \frac{1}{2}(P_2 - P_1)(V_1 + V_2)$

(4b) $= \frac{1}{2} P_1 V_1 (\Pi - 1)\left(1 + \frac{1}{\Delta}\right)$

(4c) $= \frac{1}{2} \frac{RT_1}{W} (\Pi - 1)\left(1 + \frac{1}{\Delta}\right)$

From (1) and (2) and the velocity transformations one obtains

(5) $s = \left[\frac{RT_1}{W}\left(\frac{\Pi - 1}{1 - \frac{1}{\Delta}}\right)\right]^{1/2}$

(6) $v = s\left(1 - \frac{1}{\Delta}\right)$

H can most easily be defined relative to absolute zero so that

(7) $H = \frac{H^\circ - H_0^\circ}{RT} \cdot \frac{RT}{W} = \phi \frac{RT}{W}$

For a partially dissociated gas

$$(8) \quad H = (1-\alpha)\mathcal{M}_M \frac{RT}{W} + 2\alpha \mathcal{M}_A \frac{RT}{W} + \alpha \frac{U_d}{W}$$

The perfect gas law, which is assumed throughout, has the following form

$$(9) \quad \Pi = (1+\alpha)\Delta\Theta$$

Writing $H_2 - H_1$ in terms of (7) and (8), and equating it to (4),

$$(10) \quad H_2 - H_1 = (1-\alpha)\mathcal{M}_{M2}\frac{RT_2}{W} + 2\alpha\mathcal{M}_{A2}\frac{RT_2}{W} + \alpha\frac{U_d}{W} - \mathcal{M}_{M1}\frac{RT_1}{W}$$

$$= \frac{1}{2}\frac{RT_1}{W}(\Pi - 1)\left(1 + \frac{1}{\Delta}\right)$$

Solving this and substituting (9)

$$(11a) \quad \Pi = \Theta\left[(1-\alpha)(2\mathcal{M}_{M2}-1) + 2\alpha(2\mathcal{M}_{A2}-1)\right] - (2\mathcal{M}_{M1}-1) + \frac{2\alpha U_d}{RT_1} + (1+\alpha)\frac{\Theta}{\Pi}$$

Making the substitution $\beta = 2\mathcal{M} - 1$

$$(11b) \quad \Pi = \Theta\left[(1-\alpha)\beta_{M2} + 2\alpha\beta_{A2}\right] - \beta_{M1} + \frac{2\alpha U_d}{RT_1} + (1+\alpha)\frac{\Theta}{\Pi}$$

Equations (11b), (9), (5), and (6) are used to calculate behavior in the shock wave. Some special cases of (11b) are of interest. For a pure gas with no dissociation

$$(11c) \quad \Pi = \Theta\beta_{M2} - \beta_{M1} + \frac{\Theta}{\Pi}$$

For a monotomic gas (no electronic excitation)

$$(11d) \quad \Pi = 4(\Theta - 1) + \frac{\Theta}{\Pi}$$

For a linear rigid rotor

$$(11e) \quad \Pi = 6(\Theta - 1) + \frac{\Theta}{\Pi}$$

For a non-linear rigid rotor

$$(11f) \quad \Pi = 7(\Theta - 1) + \frac{\Theta}{\Pi}$$

The same development for the case of a mixture of two gases, one inert and one dissociating, is also of interest.

$$(12)\quad H^\circ = \frac{(1-\phi)\,\mathcal{H}_I RT + \phi\left[(1-\alpha)\,\mathcal{H}_M RT + 2\alpha\,\mathcal{H}_A RT + \alpha U_d\right]}{1+\phi\alpha}$$

$$(13a)\quad \overline{W}_\alpha = \frac{(1-\phi)W_I + \phi\,(1-\alpha)\,W_M + \phi\alpha W_M}{1+\phi\alpha}$$

$$(13b)\quad = \frac{W_I + \phi(W_M - W_I)}{1+\phi\alpha}$$

$$(13c)\quad = \frac{\overline{W}}{1+\phi\alpha}$$

$$(14a)\quad H = \frac{H^\circ}{\overline{W}_\alpha}$$

$$(14b)\quad = (1-\phi)\,\mathcal{H}_I \frac{RT}{\overline{W}} + \phi\left[(1-\alpha)\,\mathcal{H}_M \frac{RT}{\overline{W}} + 2\alpha\,\mathcal{H}_A \frac{RT}{\overline{W}} + \frac{\alpha U_d}{\overline{W}}\right]$$

$$(15)\quad H_2 - H_1 = (1-\phi)\left(\mathcal{H}_{I2}\frac{RT_2}{\overline{W}} - \mathcal{H}_{I,}\frac{RT_1}{\overline{W}}\right)$$

$$+ \phi\left[(1-\alpha)\,\mathcal{H}_{M2}\frac{RT_2}{\overline{W}} + 2\alpha\,\mathcal{H}_{A2}\frac{RT_2}{\overline{W}} + \frac{\alpha U_d}{\overline{W}} - \frac{\mathcal{H}_{M1}RT_1}{\overline{W}}\right]$$

$$= \frac{1}{2}\frac{RT_1}{\overline{W}}(\Pi - 1)\left(1 + \frac{1}{\Delta}\right)$$

In this case the perfect gas law becomes

$$(16)\quad \Pi = (1+\phi\alpha)\,\Delta\Theta$$

Solving (15) and substituting (16)

$$(17a)\quad \Pi = (1-\phi)(\beta_{I2}\Theta - \beta_{I1}) + \phi\left\{\left[(1-\alpha)\beta_{M2} + 2\alpha\beta_{A2}\right]\Theta - \beta_{M1} + \frac{2\alpha U_d}{RT_1}\right\} + (1+\phi\alpha)\frac{\Theta}{\Pi}$$

$$(17b)\quad \Pi = (\beta_{I2}\Theta - \beta_{I1}) + \phi\left[(\beta_{M2} - \beta_{I2})\Theta - (\beta_{M1} - \beta_{I1}\right] + \phi\alpha\left[(2\beta_{A2} - \beta_{M2})\Theta + \frac{2U_d}{RT_1}\right] + (1+\phi\alpha)\frac{\Theta}{\Pi}$$

In the same manner one may find the expression for a mixture of an inert gas and a gas partially dissociated which dissociates further in the shock. This is probably the most complicated system in which any useful kinetics could be done.

$$(18)\quad \pi = \frac{(1-\phi)}{(1+\phi\alpha_1)}(\beta_{I2}\theta-\beta_{I1}) + \frac{\phi}{(1+\phi\alpha_1)}\left\{\left[(1-\alpha_2)\beta_{M2} + 2\alpha_2\beta_{R2}\right]\theta - \left[(1-\alpha_1)\beta_{M1} + 2\alpha_1\beta_{R1}\right] + 2(\alpha_2-\alpha_1)\frac{U_d}{RT_1}\right\} + \left(\frac{1+\phi\alpha_2}{1+\phi\alpha_1}\right)\frac{\theta}{\pi}$$

Finally, for a mixture of an inert gas and an ionizing monatomic gas

$$(19)\quad \pi = (1-\phi)(\beta_{I2}\theta-\beta_{I1}) + \phi\left\{4\left[(1+\alpha)\theta-1\right] + \frac{2\alpha U_i}{RT_1}\right\} + (1+\phi\alpha)\frac{\theta}{\pi}$$

This assumes that a gas of ions behaves as a perfect gas. In all of the last three cases the proper mean molecular weight, $\overline{W}_\alpha$ (see (13)), must be used in (5) when calculating the velocity.

For cases where ϕ is large the calculations for the shock behavior are best utilized by plotting lines of equal α, equal s, and equal v on a diagram of π versus T_2 for a given T_1, usually 300°K,* and plotting lines of equal α on a Δ versus s plot. A particular shock wave will follow along a line of constant shock velocity, s, provided that the gas comes to

---

* The final parameters are related to a given final temperature and are insensitive to the initial temperature being changed by about one percent, to the accuracy required in these experiments.

its high temperature equilibrium before the cold front.

In the case where ϕ is small (of the order of 0.01) the simplest procedure is to solve for the behavior as a function of temperature for the pure inert gas, and for the mixture with $\phi = 0.01$ and $\alpha = 0.00$, 0.50, and 1.00. From these two sets of data calculate

(20a) $$\delta\Pi = \Pi_{\phi=0.01} - \Pi_{\phi=0}$$

(20b) $$\delta\Delta = \Delta_{\phi=0.01} - \Delta_{\phi=0}$$

(20c) $$\delta v = v_{\phi=0.01} - v_{\phi=0}$$

(20d) $$\delta s' = s'_{\phi=0.01} - s'_{\phi=0}$$

where s' is defined as the velocity which the gas would have had had it had a molecular weight W_I rather than $\overline{W}$, that is

(21) $$s' = s\left(\frac{\overline{W}}{W_I}\right)^{1/2}$$

In a given shock s is measured and ϕ is calculated from the original conditions. From these s' is calculated, and then $s_{\phi=0}$ is calculated.

(22) $$s_{\phi=0} = s' - \frac{\phi}{0.01}\,\delta s'$$

$s_{\phi=0}$ is the velocity a shock wave in pure gas would have had if this same temperature had been produced. From $s_{\phi=0}$ and the careful calculations for the pure gas the temperature can be found. Since δ's have been calculated for several α's (and are approximately linear in α) the temperature for any α along the course of the reaction behind the shock can be found. Knowing the temperature at any α along the shock the true Δ, etc. can be calculated,

(23) $$\Delta_\phi = \Delta_{\phi=0} + \frac{\phi}{0.01}\,\delta\Delta \qquad \text{etc.,}$$

since the δ's are given as functions of the temperature. In mixtures of iodine and nitrogen sample calculations have shown that the δ's are linear in ϕ, up to at least $\phi = 0.02$, to the accuracy required for these experiments.

To use the observed density changes as a function of time to study the kinetics of a reaction it must be realized that there is an apparent time contraction in the moving shock wave. Consider a shock wave traveling a distance dx. The shock wave requires $dt_{shock} = \frac{dx}{s}$ to reach x + dx from x. The moving gas

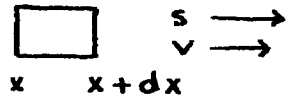

requires $dt_{real} = \frac{dx}{v}$ to reach x + dx from x. However, the observed time after the shock front reaches x + dx that the gas which was shocked at x reaches x + dx is $dt_{observed} = \frac{dx}{v} - \frac{dx}{s} = dt_{real} - dt_{shock}$. Recalling equation (6) and eliminating dx, one obtains

(24) $$dt_{real} = dt_{observed} \cdot \Delta \qquad \text{or}$$
$$dt = \Delta \, d\tau$$

The relation between the original pressure in the low pressure side of the shock tube and that in the high pressure side to the characteristics of the shock wave is given by

(25) $$v = \frac{2 a_3}{\gamma_3 - 1} \left[1 - \left(\frac{\Pi}{B} \right)^{\frac{\gamma_3 - 1}{2\gamma_3}} \right]$$

This has been repeatedly derived in the literature (17). This is not an experimentally exact formula since the mechanical process of breaking a membrane is not perfect, but it is useful for estimating the correct initial conditions to obtain a desired shock.

Appendix C

Calculation of

High Temperature Extinction Coefficients

The measurement of extinction coefficients at high temperatures is quite direct. The fraction by which the transmitted light decreases across the shock front, $\frac{i_2}{i_1}$, is measured from the oscilloscope trace. The fraction of the incident light that was transmitted by the colored gas before the shock was run, $\frac{i_1}{i_0}$, is calculated from a knowledge of ϵ at room temperature and the initial concentration of colored gas, that is,

$$\log \frac{i_1}{i_0} = -\epsilon_1 c_1 l$$

The shock parameters are determined from a measurement of the velocity of the shock so that Δ is known. Then

$$\epsilon_2 = -\frac{1}{\Delta c_1 l} \log \frac{i_2}{i_1} \frac{i_1}{i_0}$$

$$= -\frac{1}{c_2 l} \log \frac{i_2}{i_0}$$

If a reaction occurs in the gas the trace can be extrapolated visually to the initial value except in very hot shocks where the reaction is very fast and ϵ_2 cannot be measured.

Appendix D

Kinetics of the Dissociation of a Diatomic Gas in a Shock Tube

In a mixture of a dissociating diatomic gas and an inert gas the dissociation is governed by the following differential equation, which is for constant volume.

$$(1) \quad -\frac{\partial M}{\partial t}\Big|_D = k_{DM} M M + k_{DA} M A + k_{DI} M I - \left(k_{RM} A^2 M + k_{RA} A^2 A + k_{RI} A^2 I \right)$$

From a consideration of thermodynamic equilibrium it holds that for any third body

$$(2) \quad K = \frac{A^2}{M} = \frac{k_D}{k_R}$$

Combining (1) and (2) and factoring

$$(3) \quad -\frac{\partial M}{\partial t}\Big|_D = \left(K M - A^2 \right) \left(k_{RM} M + k_{RA} A + k_{RI} I \right)$$

If c_1 is the original total formal concentration of gas, and c the total formal concentration in the shocked gas, then

$$(4a) \quad c = \Delta c_1$$

$$(4b) \quad M = (1-\alpha)\, \phi c_1 \Delta$$

$$(4c) \quad A = 2\alpha\, \phi\, c_1 \Delta$$

$$(4d) \quad I = (1-\phi)\, c_1 \Delta$$

$$(5) \quad -\frac{\partial M}{\partial t}\Big|_\Delta = \phi\, c_1 \Delta \frac{d\alpha}{dt}$$

Substituting (4) and (5) in (3)

$$(6) \quad \frac{d\alpha}{dt} = \left[K \Delta c_1 (1-\alpha) - 4\phi (\Delta c_1)^2 \alpha^2 \right] \cdot \left[(2k_{RA} - k_{RM})\alpha\phi + k_{RM}\phi + (1-\phi) k_{RI} \right]$$

At this point the photometric equations will be introduced.

$$(7) \quad \epsilon\, c_{abs}\, l = -\log \frac{i}{i_0}$$

where c_{abs} is the concentration of the absorbing species. In the case of iodine or bromine, where molecules are the absorbing species, $c_{abs} = M = (1-\alpha)\phi\Delta c_1$ so that

(8) $$(1-\alpha)\,\phi\,\Delta\, c_1\, \epsilon\, l = -\log \frac{i}{i_o}$$

Taking derivatives of both sides of (8)

(9a) $$\phi\Delta c_1 \epsilon l \left[1 - (1-\alpha)\left(\frac{d\ln\Delta}{d\alpha} + \frac{d\ln\epsilon}{d\alpha}\right)\right]\frac{d\alpha}{dt} = \frac{d \log i/i_o}{dt}$$

In the case where the atoms are the absorbing species this becomes

(9b) $$2\phi\Delta c_1 \epsilon l \left[1 + \alpha\left(\frac{d\ln\Delta}{d\alpha} + \frac{d\ln\epsilon}{d\alpha}\right)\right]\frac{d\alpha}{dt} = -\frac{d \log i/i_o}{dt}$$

It can be seen from these that the case where the atoms are the absorbing species is the more desirable, because the change in light absorption due to the density increase with dissociation and that due to dissociation enhance each other.

Equations (6) and (8) are now combined and the correction for the apparent time contraction is introduced

(10) $$\left\{\left[(2k_{RA} - k_{RM})\alpha + k_{RM}\right]\phi + (1-\phi)k_{RI}\right\} = \frac{d \log i/i_o}{d\tau} \cdot \frac{1}{c_1 \Delta^2 \epsilon l \left[K\phi\Delta c_1 (1-\alpha) - 4(\phi\Delta c_1)^2\alpha^2\right]} \cdot \frac{1}{\left[1 - (1-\alpha)\left(\frac{d\ln\Delta}{d\alpha} + \frac{d\ln\epsilon}{d\alpha}\right)\right]}$$

If α can be determined at each point on the curve of $\log \frac{i}{i_o}$ the equilibrium constants can be determined, since in any shock once s is known α is known as a function of T, and Δ, K, and ϵ are assumed to be known as functions of T beforehand, and hence also of α. This expression is valid in any case, but in cases where ϕ is small changes in Δ, K, and ϵ can be approximated as linear functions of α and an expression formed

which can be integrated. In the case where ϕ is large equation (10) would have to be used since Δ, κ, and ϵ could not be approximated by linear expressions. If this were the case k_{RI} would probably be known, so that k_{RA} and k_{RM} alone would need to be determined. The above method requires that α be known at each point, but if Δ, κ, and ϵ are known as functions of α, then given the shock velocity the value of $\log \frac{i}{i_o}$ for a given α could be calculated, and all that need be determined experimentally is the time dependence of $\log \frac{i}{i_o}$.

To determine the values of ϵ and k_{RI} as functions of temperature experiments where ϕ is small (about 0.01) must be carried out. In this case i is plotted versus τ and extrapolated to zero time. From this one can calculate $\left(\log \frac{i}{i_o}\right)_{\tau=0}$.

$$(11) \qquad \frac{\log i/i_o}{(\log i/i_o)_{\tau=0}} = (1-\alpha)\frac{\Delta \epsilon}{\Delta_{\tau=0}\epsilon_{\tau=0}}$$

For small ϕ the changes in Δ and ϵ can be approximated as linear with α, that is

$$(12) \qquad \Delta = \Delta_{\tau=0}\left(1 + \frac{d\ln\Delta}{d\alpha}\alpha\right) \text{ where } \frac{d\ln\Delta}{d\alpha} \text{ is assumed constant}$$

$$\epsilon = \epsilon_{\tau=0}\left(1 + \frac{d\ln\epsilon}{d\alpha}\alpha\right) \text{ where } \frac{d\ln\epsilon}{d\alpha} \text{ is assumed constant}$$

so that

$$(13) \qquad \frac{\log i/i_o}{(\log i/i_o)_{\tau=0}} = (1-\alpha)\left(1 + \frac{d\ln\Delta}{d\alpha}\alpha\right)\left(1 + \frac{d\ln\epsilon}{d\alpha}\alpha\right)$$

This can be solved for α by successive approximations.

Equation (10) now becomes

$$(14) \qquad k_{RI} = \frac{d\log i/i_o}{d\tau} \cdot \frac{1}{\Delta^2 C_1 \epsilon \ell \left[\kappa\phi\Delta C_1 (1-\alpha) - 4(\phi\Delta C_1)^2\alpha^2\right]} \cdot \frac{1}{1 - (1-\alpha)\left(\frac{d\ln\Delta}{d\alpha} + \frac{d\ln\epsilon}{d\alpha}\right)}$$

which can be solved as before. If it is desired to integrate it is better to go back to equation (6) which becomes (allowing for the time correction also)

$$(15)\qquad \frac{d\alpha}{d\tau} = k_{RI}\frac{\Delta}{\phi}\left[K\phi\Delta C_1(1-\alpha) - 4(\phi\Delta C_1)^2\alpha^2\right]$$

$$(16)\qquad \frac{d\alpha}{d\tau} = k_{RI}\frac{\Delta^3}{\phi}\left[\phi C_1\frac{K}{\Delta}(1-\alpha) - 4(\phi C_1)^2\alpha^2\right]$$

Using equations (12) and a similiar expression for K, and making certain approximations by the binomial expansion, (16) becomes

$$(17)\qquad \frac{d\alpha}{d\tau} = k_{RI}\frac{\Delta_o^3}{\phi}(1+\zeta\alpha)\left[\frac{K_o}{\Delta_o}\phi C_1(1+\eta\alpha)(1-\alpha) - 4(\phi C_1)^2\alpha^2\right]$$

where $$\zeta = 3\frac{d\ln\Delta}{d\alpha}$$

$$\eta = \frac{d\ln K}{d\alpha} - \frac{d\ln\Delta}{d\alpha} - \frac{3}{4}\frac{d\ln K}{d\alpha}\frac{d\ln\Delta}{d\alpha}$$

Let $\xi = \frac{4\phi C_1\Delta_o}{K_o}$ and (17) can be written

$$(18a)\qquad \frac{d\alpha}{K_o\Delta_o^2 C_1(1+\zeta\alpha)\left[1-(1-\eta)\alpha-(\xi+\eta)\alpha^2\right]} = k_{RI}\,d\tau$$

Integrating and rearranging this

$$(18b)\qquad \frac{-1}{K_o\Delta_o^2 C_1}\left\{\frac{1}{\left[1+\frac{4(\xi+\eta)}{(1-\eta)^2}\right]^{1/2}}\left[\frac{1-\frac{\zeta(1-\eta)}{2(\xi+\eta)}}{(1-\eta)\left(1-\frac{\zeta^2}{\xi+\eta}-\zeta\frac{(1-\eta)}{\xi+\eta}\right)}\right]\right.$$

$$\ln\left[\frac{-\alpha-\frac{1-\eta}{2(\xi+\eta)}\left(1-\sqrt{\ }\right)}{\alpha+\frac{1-\eta}{2(\xi+\eta)}\left(1+\sqrt{\ }\right)}\right] - \left[\frac{\frac{\zeta}{\xi+\eta}}{1-\frac{\zeta^2}{\xi+\eta}-\frac{\zeta(1-\eta)}{\xi+\eta}}\right]$$

$$\left.\ln\frac{\left[1-(1-\eta)\alpha-(\xi+\eta)\alpha^2\right]^{1/2}}{1+\zeta\alpha}\right\} = k_{RI}\tau + \text{constant}$$

Expressing (18b) in terms of the equilibrium α

$$\alpha_\infty = \frac{-(1-\eta)}{2(\xi+\eta)}\left(1 - \sqrt{1 + \frac{4(\xi+\eta)}{(1-\eta)^2}}\right)$$

if $\xi+\eta = 0$ $\qquad \alpha_\infty = \frac{1}{1-\eta}$

(18c)
$$\frac{-1}{K_0 \Delta_0^2 c_1}\left\{\frac{1}{\left[1 + \frac{4(\xi+\eta)}{(1-\eta)^2}\right]^{1/2}}\left[\frac{2(\xi+\eta) - \int(1-\eta)}{2(1-\eta)\left[(\xi+\eta) - \int^2 - \int(1-\eta)\right]}\right]\right.$$

$$\ln\frac{\alpha_\infty - \alpha}{(1-\eta) + (\xi+\eta)(\alpha_\infty + \alpha)} - \left[\frac{\int}{(\xi+\eta) - \int^2 - \int(1-\eta)}\right]$$

$$\left.\ln\frac{\left[(\alpha_\infty - \alpha)\left[(1-\eta) + (\xi+\eta)(\alpha_\infty - \alpha)\right]\right]^{1/2}}{1 + \int\alpha}\right\} = k_{RI}\,\tau + \text{constant}$$

The above equation was rather tedious to use and it was found that a measurement of the initial slope of the reaction gave satisfactory results more readily. The calculations based on the initial slope were made as follows;

For $\alpha = 0$ equation (6) becomes

(19) $$\frac{d\alpha}{dt} = K \Delta c_1 \left(\phi\, k_{RM} + (1-\phi)\, k_{RI}\right)$$

Let $$k = \phi\, k_{RM} + (1-\phi)\, k_{RI}$$

then (19) can be written

(20) $$k = \frac{d\alpha}{dt}\,\frac{1}{K \Delta c_1}$$

$$= \frac{\dfrac{d \log i/i_0}{d\tau}}{\dfrac{d \log i/i_0}{d\alpha}}\;\frac{1}{K \Delta^2 c_1}$$

Recall

(8) $$\log \frac{i}{i_0} = -\epsilon \Delta \phi c_1 \ell (1-\alpha)$$

which becomes, upon differentiation with respect to α

(21) $$\frac{d \log i/i_0}{d\alpha} = \left(1 - \frac{1}{\Delta}\frac{d\Delta}{d\alpha} - \frac{1}{\epsilon}\frac{d\epsilon}{d\alpha}\right)\log\frac{i}{i_0} = -Q \log\frac{i}{i_0}$$

If $\frac{1}{\log i/i_0}$ is plotted versus τ the slope is $\frac{-1}{(\log i/i_0)^2}\,\frac{d \log i/i_0}{d\tau}$

so that

$$(22) \qquad P_2 = \frac{\text{slope} \times (\log i/i_0)}{Q K \Delta^2 c_1} = \frac{\text{slope}}{\text{intercept}} \frac{1}{Q K \Delta^2 c_1}$$

The derivatives needed above can be found by differentiating equations (16), (17), and (5) from Appendix B to obtain the results

$$(23) \quad \frac{d\theta}{d\alpha} = \frac{-\phi\theta\left\{\left(\Delta - \frac{1}{\pi}\right) + \left(\Delta - 2 + \frac{1}{\pi}\right)\left[\left(2\beta_{A2} - \beta_{M2}\right) + \frac{2U_d}{RT_1\theta}\right]\right\}}{(1+\phi\alpha)\left(\Delta - \frac{1}{\pi}\right) + \left(\Delta - 2 + \frac{1}{\pi}\right)\left[(1-\phi)\beta_{I2} + \phi[(1-\alpha)\beta_{M2} + 2\alpha\beta_{A2}]\right.}$$

$$(24) \quad \frac{d\Delta}{d\alpha} = \frac{\phi\left\{\Delta(\Delta-1)\left(\left[\left(2\beta_{A2} - \beta_{M2}\right) + \frac{2U_d}{RT_1\theta}\right] - [(1-\phi)\beta_{I2} + \phi[(1-\alpha)\beta_{M2} + 2\alpha\beta_A\right.\right.}{\text{same denominator}}$$

$\frac{d\epsilon}{dT}$ is determined experimentally from the ϵ versus T curves and

$$(25) \qquad \frac{d\epsilon}{d\alpha} = \frac{d\epsilon}{dT_2} T_1 \frac{d\theta}{d\alpha}$$

References

(1) Tucker Carrington and Norman Davidson, Journal of Physical Chemistry (1953), 57, 418.

(2) Doyle Britton, Norman Davidson, and Garry Schott, Discussions of the Faraday Society (1954), no. 17, 58.

(3) W. Döring, Annalen der Physik (1949), 6 5, 133.

(4) W. B. DeMore and N. Davidson, private communication.

(5) Garry Schott, private communication.

(6) Edward F. Smiley and Ernst H. Winkler, Journal of Chemical Physics (1954), 22, 2018.

(7) A. P. Acton, R. G. Aicken and N. S. Bayliss, Journal of Chemical Physics (1936), 4, 474.

(8) N. S. Bayliss and A. L. G. Rees, Transactions of the Faraday Society (1939), 35, 792.

(9) Henry Margenau and George Mosely Murphy, "The Mathematics of Chemistry and Physics," New York, 1943, p. 502.

(10) M. I. Christie, R. G. W. Norrish, and G. Porter, Proceedings of the Royal Society (1952), A 216, 152.

(11) Royal Marshall and Norman Davidson, Journal of Chemical Physics (1953), 21, 659.

(12) K. E. Russell and J. Simons, Proceedings of the Royal Society (1953), A 217, 271.

(13) Robert L. Strong and John E. Willard, Abstracts of Papers Presented at New York, N. Y., Sept. 12 to Sept. 17, 1954, American Chemical Society Meeting, p. 26R.

(14) M. Christie, R. G. W. Norrish and G. Porter, Discussions of the Faraday Society (1954), 17, 107.

(15) Don L. Bunker, private communication.

(16) E. Rabinowitch and W. C. Wood, Transactions of the Faraday Society (1936), 32, 907.

(17) W. Payman and W. C. F. Shepherd, Proceedings of the Royal Society (1946), A 186, 293.

(18) National Bureau of Standards, "Selected Values of Chemical Thermodynamic Properties, Series III," Washington, D. C., 1954.

Propositions

1. It is suggested that the kinetics of the decomposition of the carbonyl halides be studied using the shock wave technique.

2. Certain disubstituted compounds of ferrocene have been prepared which are thought to be substituted on opposite rings as far apart as possible (1).

(a) It is suggested that a determination of the space group of one of these crystalline compounds might confirm this conclusion by showing that a center of symmetry is required in the molecule.

9 (b) It is suggested that if ferrocene diacetic acid be prepared, from this compound it might be possible to obtain information about the location of the groups or the energy of rotation of one ring with respect to the other by a study of the formation of the acid anhydride.

(1) R. B. Woodward, M. Rosenblum, and M. C. Whiting, J.A.C.S., 74, 3458 (1952).

3. It is suggested that the structures of fifth group pseudohalides be determined with the end of explaining the unusual behavior of some of these compounds. In particular the structures of the triisocyanates of phosphorus, antimony, and arsenic (1, 2) and of phosphorus tri- and pentacyanide (3) should be determined. From a consideration of possible resonance forms it is suggested that these molecules might be planar, as compared to the phosphorus trihalides which are pyramidal.

(1) G. S. Forbes and H. H. Anderson, J. A. C. S., 62, 761 (1940).
(2) H. H. Anderson, J.A.C.S., 64, 1757 (1942).
(3) H. Gall and J. Schuppen, Ber, 63B, 482 (1930).

4. Light rare earth sulfates crystallize as enneahydrates, while heavy rare earth sulfates crystallize as octahydrates, the change presumably because the heavy rare earth ions cannot support the coordination number of twelve which is required for one half the metal ions in the enneahydrate structure (1). The other half of the metal ions in this structure have nine fold coordination.

It is suggested that the compound $LaY(SO_4)_3 \cdot 9H_2O$ should be prepared if possible, and examined to see if the metal ions are ordered between the two different crystallographic positions.

(1) E. B. Hunt Jr., R. E. Rundle, and A. J. Stosick, Acta Cryst., 7, 106 (1954).

5. PBr_5 is strongly colored in solution, and in 0.01 F solution in CCl_4 only about one third dissociated. Because of the strong color it might be suspected that there is a molecular compound of some sort rather than molecular PBr_5.

It is suggested that this could be determined by finding

the position of the phosphorus K absorption edge in this solution.
(1) A. I. Popov and N. E. Skelly, J. A. C. S., 76, 3916 (1954)

6. It is suggested that the compound 1,2,5,6-cyclo-octatetraene should be prepared if possible. It would offer an interesting example for the study of pi bond interaction in a non-conjugated system. It would have three more or less strain free isomers, d, l, and meso which would differ by rotation around one or two double bonds and which therefore would be separable isomers.

7. It is suggested that the decomposition of 1,2-diiodo-ethane should be studied by the shock tube method. This reaction has been studied at low temperatures (1) and the high temperature results would provide knowledge of a unimolecular reaction over a large temperature range.
(1) L. B. Arnold and G. B. Kistiakowsky, J. Chem. Phys., 1, 166 (1933).

8. It has been shown by radioactive exchange studies that Cl_2 exchanges rapidly with equatorial Cl and slowly with apical Cl in PCl_5 (1).
It is suggested that the following exchange reactions be studied, F_2-PF_5, Cl_2-PF_3Cl_2, F_2-PF_3Cl_2, in the same manner.
(1) J. J. Downs and R. E. Johnson, J.A.C.S., 77, 2008 (1955).

9. It is suggested that benzene hexacarboxylic acid (mellitic acid) is a compound which might be completely intramolecularly hydrogen bonded, and that these might be symmetric hydrogen bonds. Crystal structure studies by x-ray and neutron diffraction should be made to determine whether this is so.

10. The arguments of Perros et al. (1) that PrF_4 should be stable are incorrect. A correct argument says that the free energy of the reaction

$$PrF_{3(c)} + \tfrac{1}{2}F_{2(g)} \rightarrow PrF_{4(c)} \qquad \text{equals } -1 \pm 24$$

kcal/mole. All attempts to fluorinate PrF_3 have been unsuccessful, but it is suggested that it might be possible to make +4 Pr in a fluoride by fluorinating solid solutions of PrF_3 in CeF_3.
(1) T. P. Perros, T. R. Munson, and C. R. Naeser, J. Chem. Educ., 30, 402 (1953).